# Effective single-band models for the high-$T_c$ cuprates. I. Coulomb interactions

L. F. Feiner
*Philips Research Laboratories, Prof. Holstlaan 4, 5656 AA Eindhoven, The Netherlands*

J. H. Jefferson and R. Raimondi
*DRA Electronics Sector, St. Andrews Road, Great Malvern, Worcestershire WR14 3PS, England*

(Received 3 January 1995; revised manuscript received 19 July 1995)

Starting with the three-band extended Hubbard model (or $d$-$p$ model) widely used to represent the $CuO_2$ planes in the high-$T_c$ cuprates, we make a systematic reduction to an effective single-band model using a previously developed cell-perturbation method. The range of parameters for which this mapping is a good approximation is explored in the full Zaanen-Sawatzky-Allen diagram (copper Coulomb repulsion $U_d$ versus charge-transfer energy $\varepsilon$), together with an investigation of the validity of a further mapping to an effective charge-spin ($t$-$J$-$V$) model. The variation of the effective single-band parameters with the parameters of the underlying multi-band model is investigated in detail, and the parameter regime where the model represents the high-$T_c$ cuprates is examined for specific features that might distinguish it from the general case. In particular, we consider the effect of Coulomb repulsions on oxygen ($U_p$) and between copper and oxygen ($V_{pd}$). We find that the reduction to an effective single-band model is generally valid for describing the low-energy physics, and that $V_{pd}$ and $U_p$ (unless unrealistically large) actually slightly improve the convergence of the cell-perturbation method. Unlike in the usual single-band Hubbard model, the effective intercell hopping and Coulomb interactions are different for electrons and holes. We find that this asymmetry, which vanishes in the extreme Mott-Hubbard regime ($U_d \ll \varepsilon$), is quite appreciable in the charge-transfer regime ($U_d > \varepsilon$), particularly for the effective Coulomb interactions. We show that for doped holes (forming Zhang-Rice singlets) on neighboring cells the interaction induced by $V_{pd}$ can even be attractive due to locally enhanced $pd$ hybridization, while this cannot occur for electrons. The Coulomb interaction induced by $U_p$ is always repulsive; in addition $U_p$ gives rise to a ferromagnetic spin-spin interaction which opposes antiferromagnetic superexchange. We show that for hole-doped systems this leads to a subtle cancellation of attractive and repulsive contributions, due to antiferromagnetic and charge-polarization effects, to the net static interaction in a charge-spin ($t$-$J$-$V$) model, and we discuss the significance of this result. The asymmetry in the $ee$, $hh$, and $eh$ effective hopping parameters can be particularly large for next-nearest neighbors. Specializing to cuprate parameters, we find that the asymmetry in the nearest-neighbor hopping parameters almost vanishes (accidentally), while the next-nearest-neighbor hopping parameter $t'$ is close to zero for electrons but is appreciable for holes ($t' \approx -0.06$ eV). The effective Coulomb interaction between doped holes is found to be repulsive, and even slightly larger than for electrons. *All* the underlying $d$-$p$ parameters make significant contributions to the effective interactions and it is shown that certain approximations, such as $U_d = \infty$ and $t_{pp} = 0$, can be qualitatively incorrect.

## I. INTRODUCTION

Since the discovery of high-$T_c$ superconductivity, there has been a great deal of discussion about the choice of an effective model suitable to describe the properties of the copper oxide planes in the perovskite structure. Anderson[1] conjectured that a single-band Hubbard model may be the route to understanding the origin of the unusual behavior of these materials. In the regime of strong correlations ($U \gg t$), the Hubbard model reduces to the so called $t$-$J$ model, with the exchange interaction $J$ arising in second order in perturbation theory, $J = 4t^2/U$. The validity of an effective single-band model was questioned by Emery[2] following convincing experimental evidence that mobile holes go predominantly in oxygen $2p_x$ and $2p_y$ orbitals.[3,4] He proposed a three-band extended Hubbard model (often referred to as the Emery model) and went on to describe processes, based on strong-coupling perturbation theory, which did not appear to have an analog in the single-band description. A similar model was proposed by Varma *et al.*,[5] who emphasized the importance of charge-transfer excitations.

However, Zhang and Rice[6] showed, at least in the limit of sufficiently large Coulomb copper repulsion ($U_d$) and charge-transfer energy ($\varepsilon = \varepsilon_p - \varepsilon_d$), that the Emery model does indeed reduce to an effective single-band model for the low-energy physics because doped holes would form local singlets. Although their treatment was again based on strong-coupling perturbation theory (and neglected Coulomb repulsions on oxygen, between oxygen and copper, and the oxygen bandwidth), which, as demonstrated explicitly by Eskes and Jefferson,[7] is clearly not valid for realistic parameter values, the concept of local [Zhang-Rice (ZR)] singlets nevertheless *is* valid. Indeed, impurity calculations[8] as well as exact calculations on finite clusters[9,10] have demonstrated that the ZR singlets are well separated in energy from a manifold of higher-lying two-hole states.[8] Further support for the equivalence of a single-band description came from exact diagonalizations of small clusters which showed directly, by

 

suitably fitting the parameters of the single-band model, that the low-energy states could be made to match closely those of the Emery model.[10–12] This was taken further by Batista and Aligia who combined results on finite clusters with a strong-coupling canonical expansion of the Emery model to get improved estimates of the effective parameters.[13]

A more explicit derivation was given by Jefferson, Eskes, and Feiner[14] and independently by Lovtsov and Yushankhai[15] and by Schüttler and Fedro[16] by means of the cell-perturbation method introduced by Jefferson.[17] The great advantage of this approach is that, unlike the conventional perturbation approach, it is highly convergent, giving accurate results in second order over a wide range of parameters. A further advantage is that the method also generates explicitly all terms of the effective single-band Hamiltonian, showing unequivocally the occurrence of residual interactions between the effective particles in the single-band model. This could be relevant, for example, in identifying interactions, absent in the ordinary Hubbard model, which might give rise to superconductive pairing. This controversial issue is of current interest in view of the apparent absence of superconductivity in the ordinary Hubbard model as demonstrated by quantum Monte Carlo studies,[18,19] with similar studies,[20] as well as mean-field approaches,[21–23] indicating that a superconducting phase does occur in the Emery model.

Since its introduction, the cell approach has been further exploited for various purposes. This has included estimations of triplet admixtures into the ZR singlets,[24,25] an investigation of residual effective hole-hole interactions,[26] a more accurate estimate of $\varepsilon$ for the cuprates in the presence of additional Coulomb repulsions (on-site oxygen $U_p$ and copper-oxygen $V_{pd}$),[27,28] an investigation of the influence of those Coulomb interactions on the metal-insulator transition,[29,30] and an analysis of the relation between the single-particle spectra in the Emery model and in the effective single-band model.[31]

Nevertheless, the issue of the validity of an effective single-band description has remained controversial (see, e.g., the discussion in Refs. 19,32), in particular if the $d \rightarrow p$ charge-transfer excitations promoted by $V_{pd}$ were important,[5] since the oxygen degrees of freedom are in a sense integrated out in going to the single-band model, and this issue is taken up in the present paper. The above investigations focused mainly on the particular set of parameters appropriate for the cuprates. In the present work we take a somewhat different perspective and explore the range of parameters in extended Hubbard models for which a mapping to an effective single-band model or, more restrictively, an effective charge-spin model, may be justified by the cell-perturbation method. This includes the metallic as well as the insulating side of the Mott transition. In particular, we ask whether the low-energy physics of charge-transfer (CT) systems is basically equivalent to that of Mott-Hubbard (MH) systems *in general*, or just for a selected parameter regime in the Zaanen-Sawatzky-Allen (ZSA) phase diagram.[33] One motivation is to possibly find a clue for high-$T_c$ superconductivity by ascertaining what, if anything, is special about the cuprates. Do they behave effectively like a Hubbard system while an arbitrary CT system would not, or is it, for example, that the residual interactions after mapping on a Hubbard model are unusually strong? We also present a detailed investigation of the effect of the various Coulomb repulsion terms ($U_d$, $U_p$, and $V_{pd}$) on the parameters of the effective single-band model, with simple arguments (and expressions) which highlight the physics behind the effects they produce. This extends our previous treatment[14] for which $U_d = \infty$ and $U_p = V_{pd} = 0$.

The plan of the paper is as follows. In Sec. II we briefly recapitulate the cell approach showing how the original multi-band model may be expressed in the cell basis. In Sec. III we outline the derivation of an effective single-band model, stressing the similarities and differences to the usual Hubbard model and exploring the range of parameters for which such a mapping may be justified. We investigate in particular whether the mapping can break down because of the presence of the "Emery-Reiter triplet"[34] or the Frenkel-type charge-transfer exciton.[31] The mapping is actually from a two-band model which includes only one orbital on copper ($3d_{x^2-y^2}$) and one "molecular" orbital on the surrounding oxygen ions which transforms in the same way (i.e., like $b_1$). The validity of this restriction to two bands will be discussed in the following companion paper,[35] henceforth referred to as II, where we consider further orbitals, including $p_z$ orbitals on apical oxygen. In Sec. III we also make a detailed investigation of the dependence of the parameters of the effective models on those of the original two-band model. This includes the effective hopping parameters, the superexchange, and the residual effective Coulomb interactions. In particular we investigate the physical consequences of varying the Coulomb repulsion terms ($U_d$, $U_p$, and $V_{pd}$) together with the charge-transfer energy $\varepsilon$ and oxygen bandwidth. For the effective single-band model this includes the metallic as well as the insulating side of the metal-insulator (Mott) transition and a discussion of the asymmetry between electron and hole doping. Here we discuss in detail the remarkable result that the effective Coulomb interaction between doped holes can be attractive due to the hybridized nature of the ZR singlets, while the interaction between doped electrons is invariably repulsive, to which we recently drew attention.[36] A further reduction of the effective single-band model, to an effective charge-spin model, is performed in Sec. IV where it is shown that the range of initial parameters for which this is justified is significantly more restrictive. Finally, in Sec. V we summarize the main results and discuss their implications. Mathematical details are collected in the Appendices of the companion paper II.

## II. HAMILTONIAN IN THE CELL BASIS

We start with a multi-band, tight-binding model for the Cu-O planes of the high-temperature superconductors, which includes orbitals on both copper and oxygen. Only nearest-neighbor Cu-O and O-O hopping terms are included together with on-site Coulomb repulsion (Hubbard-$U$) terms on Cu and O and between Cu and O. Relative to a "vacuum" of filled $3d$ shells on the copper and $2p$ shells on oxygen, the most important orbitals are the $3d_{x^2-y^2}(d_x)$ orbitals on Cu and $2p_x/2p_y$ $\sigma$ orbitals on O. It is believed that holes in (antibonding) hybrids of these orbitals are primarily responsible for both magnetism and conduction in the Cu-O planes, at least for hole concentrations relevant to the insulating and superconducting regimes. Since there are just three orbitals

per unit cell (i.e., a $d_x$ orbital on the Cu site with $p_x$ and $p_y$ orbitals on neighboring oxygen ions with lobes pointing towards the copper), this $d$-$p$ model is sometimes referred to as the three-band model (or as the Emery model).

The Hamiltonian[2,5] may be written in the form

$$H=\sum_i \varepsilon_i n_i+\sum_{\langle ij\rangle}\sum_\sigma t_{ij}(c^\dagger_{i\sigma}c_{j\sigma}+\text{H.c.}) + \sum_i U_i n_{i\uparrow}n_{i\downarrow}+\sum_{\langle ij\rangle} V_{ij}n_i n_j . \tag{2.1}$$

The index $i$ runs over all localized orbitals in the Cu-O plane, i.e., $c_i \equiv d_{x,i}$, the $d_x$ orbital located at copper site $i$, or $p_{x,i}(p_{y,i})$, the $p_x(p_y)$ orbital on the nearest-neighbor oxygen site to Cu site $i$ in the positive $x(y)$ direction; $\varepsilon_i=\varepsilon_d$ or $\varepsilon_p$ are the local energies on Cu and O; $t_{ij}$ are nearest-neighbor hopping matrix elements, i.e., $t_{ij}=\pm t_{pd}$ or $\pm t_{pp}$, with due regard to the phase of the orbitals (direct Cu-Cu hopping is neglected); $U_i=U_d$ or $U_p$ is the on-site Coulomb repulsion energy; and $V_{ij}=V_{pd}$ is the Coulomb repulsion energy between nearest-neighbor Cu and O ions (all other Coulomb matrix elements are neglected). In later sections we will make plots of various quantities which depend on these parameters, in which one or more are varied from a ''standard set'' typical of the cuprates. We take this standard set to be (in units of $t_{pd}\approx 1.3$ eV) $\varepsilon_p-\varepsilon_d=2.7$, $t_{pd}=1$, $t_{pp}=0.5$, $U_d=7$, $U_p=3$, and $V_{pd}=1$.[37–41]

The first stage in obtaining a representation of the Hamiltonian in the cell basis is to transform the oxygen orbitals to a form which reflects the local symmetry. Although this is readily done by forming the ''molecular'' orbitals $\frac{1}{2}(p_x-p_y-p_{-x}+p_{-y})$ (transforming like $b_1$) and $\frac{1}{2}(p_x+p_y-p_{-x}-p_{-y})$ (transforming like $a_1$), these local oxygen orbitals are not orthogonal. It is actually more convenient to transform to orthogonal (Wannier) orbitals using the ''canonical fermions'' of Shastry[42] or a variation thereof. (See Appendix A of II for further details.) The whole problem now reduces to a square planar array of ''cells,'' each of which contains three (hole) orbitals: $d_x$, $a$ (transforming like $a_1$), and $b$ (transforming like $b_1$). As pointed out by Zhang and Rice,[6] much of the essential physics is retained if we reduce this to a two-band model by simply dropping the terms involving the $a$ orbitals, since with the ''canonical'' choice for the oxygen Wannier orbitals the $d_x$ orbital on a Cu ion hybridizes only, via hopping, with the $b$ orbitals, and the $a$-$b$ coupling is weak.[14] The resulting two-band model may be written in the form $H=H_0+H_{\rm cc}$, where $H_0$ is the Hamiltonian for noninteracting cells and $H_{\rm cc}$ the cell-cell interaction. Explicitly, $H_0$ has the form $H_0=\Sigma_i h_i$, where $h$ is the Hamiltonian for a single cell:

$$h=\bar{\varepsilon}n^{(b)}-\tau\sum_\sigma (d^\dagger_{x,\sigma}b_\sigma+\text{H.c.})+U_d n^{(d)}_\uparrow n^{(d)}_\downarrow + U_b n^{(b)}_\uparrow n^{(b)}_\downarrow + V_{db}n^{(d)}n^{(b)}, \tag{2.2}$$

with $\bar{\varepsilon}=\varepsilon_p-\varepsilon_d-2\nu_{00}t_{pp}=\varepsilon_p-\varepsilon_d-1.4536t_{pp}$ (the effective charge-transfer energy of the $b$ band), $\tau=2\mu_{00}t_{pd}=1.9162\ t_{pd}$, $U_b=\psi_{0000}U_p=0.2109\ U_p$, and $V_{db}=\phi_{000}V_{pd}=0.9180\ V_{pd}$.[43] The cell-cell interaction $H_{\rm cc}$ is conveniently decomposed as

$$H_{\rm cc}=H_{\rm hopping}+H_{pd}+H_p , \tag{2.3}$$

where the three parts are

$$H_{\rm hopping}=-2t_{pd}{\sum_{ij}}'\sum_\sigma \mu_{ij}(d^\dagger_{x,i\sigma}b_{j\sigma}+b^\dagger_{i\sigma}d_{x,j\sigma}) -2t_{pp}{\sum_{ij}}'\sum_\sigma \nu_{ij}b^\dagger_{i\sigma}b_{j\sigma}, \tag{2.4}$$

$$H_{pd}=V_{pd}{\sum_{lij}}'\sum_\sigma \phi_{lij}n^{(d)}_l b^\dagger_{i\sigma}b_{j\sigma}, \tag{2.5}$$

$$H_p=U_p{\sum_{klij}}'\psi_{klij}b^\dagger_{k\uparrow}b_{l\uparrow}b^\dagger_{i\downarrow}b_{j\downarrow}, \tag{2.6}$$

where the coefficients $\mu_{ij}$, $\nu_{ij}$, $\phi_{lij}$, and $\psi_{klij}$ follow from the Wannier transformation (see Appendix A of II for further details), and the primes on the summations indicate that the intracell terms ($i=j$, $l=i=j$, and $k=l=i=j$, respectively) should be omitted, since they are already included in (2.2). It is easy to see that while the tight-binding model in the original basis [Eq. (2.1)] had only nearest-neighbor interactions, the transformed Hamiltonian has no such restriction and the summations are over all cells. This is to some extent artificial, being a consequence of the orthogonalization of the oxygen molecular orbitals, described above, which generates long-range, but quite rapidly decaying interactions. In practice we shall restrict the interaction range to nearest- and next-nearest-neighbor cells. Note that the retention of next-nearest-neighbor interactions is important and represents a real physical effect, since their main contribution comes from *direct* O-O hopping ($t_{pp}$) of the in-plane oxygen holes.

We also see directly from (2.5) and (2.6) that the transformed Hamiltonian will, in addition to the two-cell interactions, contain three- and four-cell interactions arising from the O-O and Cu-O Coulomb terms. Since the Wannier coefficients $\phi_{lij}$ and $\psi_{klij}$ are in general somewhat smaller for three- and four-cell terms than for two-cell terms ($\phi_{lij}\ll\phi_{iij}$, etc., e.g., $\phi_{1'01}=0.0296$, while $\phi_{001}=-0.1342$, where 1 denotes a cell that is nearest neighbor to cell 0), then it is tempting to drop simply all terms involving such Wannier coefficients with more than two different indices. However, this is *not* necessarily a good approach since the summation of all such terms is not small, in general, and may be comparable with the two-cell terms due to the sum rules $\Sigma_{l(\neq i,j)}\phi_{lij}=-2\phi_{iij}$ and $\Sigma_{l(\neq i,j)}\psi_{llij}=-2\psi_{iiij}$ (see Appendix A of II). We cannot apply this directly in Eqs. (2.5) and (2.6) due to the presence of the number operators $n^{(d)}_l$ and $n^{(b)}_{l\sigma}$, respectively, in the summation. However, we may assume that some ''reference'' values $\bar{n}^{(d)}$, $\bar{n}^{(b)}_\sigma$ are available for these densities, from which deviations are small or few. For example, for low doping most cells will have just one hole and one would set $\bar{n}^{(d)}=n^{(d)}_g\equiv\langle g_\sigma|n^{(d)}|g_\sigma\rangle$, etc., where $|g_\sigma\rangle$ is the one-hole ground state of the single-cell Hamiltonian $h$, Eq. (2.2). (See also below.) It is then expedient to perform the summation of the three-cell terms with all summed-over cells assumed at the reference densities, and include the result with the two-hole terms. Performing this rearrangement in Eq. (2.5) and invoking the above sum rule together with the relation $\phi_{jij}=\phi_{iij}$ yields, directly,

$$H_{pd}=V_{pd}\sum_{ij}{}'\phi_{ijj}n_i^{(d)}n_j^{(b)}$$
$$+V_{pd}\sum_{ij}{}'\sum_{\sigma}\phi_{iij}(n_i^{(d)}+n_j^{(d)}-2\bar{n}^{(d)})b_{i\sigma}^{\dagger}b_{j\sigma}$$
$$+V_{pd}\sum_{lij}{}''\sum_{\sigma}\phi_{lij}(n_l^{(d)}-\bar{n}^{(d)}\mathbb{1}_l)b_{i\sigma}^{\dagger}b_{j\sigma}, \qquad (2.7)$$

with the double prime indicating that both intracell and two-cell terms are excluded. Note that we have explicitly separated contributions which do not transfer charge (the first sum, which gives rise to effective Coulomb interactions between $d$ holes and $b$ holes) and contributions which give rise to effective hopping of $b$ holes (the second sum). These will be considered further in Secs. III E and III B, respectively. In exactly the same way we can rearrange Eq. (2.6) as

$$H_p=U_p\sum_{ij}{}'\psi_{iijj}(n_{i\uparrow}^{(b)}n_{j\downarrow}^{(b)}-b_{i\uparrow}^{\dagger}b_{i\downarrow}b_{j\downarrow}^{\dagger}b_{j\uparrow})+U_p\sum_{ij}{}'\sum_{\sigma}\psi_{iiij}(n_{i\bar{\sigma}}^{(b)}+n_{j\bar{\sigma}}^{(b)}-2\bar{n}_{\bar{\sigma}}^{(b)})b_{i\sigma}^{\dagger}b_{j\sigma}$$
$$+U_p\sum_{klij}{}''\psi_{klij}(b_{k\uparrow}^{\dagger}b_{l\uparrow}-\bar{n}_{\uparrow}^{(b)}\mathbb{1}_l\delta_{kl})(b_{i\downarrow}^{\dagger}b_{j\downarrow}-\bar{n}_{\downarrow}^{(b)}\mathbb{1}_i\delta_{ij}). \qquad (2.8)$$

We have again separated contributions which do not and which do transfer charge. The former (first sum) contains effective intercell spin interactions between holes on oxygen, in addition to effective Coulomb terms. These will be considered further in Sec. III D. The remaining three- and four-cell interactions in Eqs. (2.7) and (2.8) are expected to be weak[44] and we shall further ignore them.

The essence of the cell method is to express the two-band Hamiltonian in terms of the eigenstates of the single-cell Hamiltonian $h$ [Eq. (2.2)], which already include most of the electron correlation that results from the competition between Coulomb repulsion and $p$-$d$ hybridization. Let us denote the cell eigenstates by $|\nu\rangle$, with corresponding eigenvalues $E_\nu$. The parameter $\nu$ denotes collectively the quantum numbers for the cell eigenstate which includes the number of particles as well as the orbital and spin quantum numbers. Since there are two independent orbitals per cell, these states consist of a vacuum (zero-hole) state $|0\rangle$, two one-hole states $|g_\sigma\rangle$ and $|e_\sigma\rangle$ (doublets), three two-hole singlet states $|S\rangle$, $|S'\rangle$, and $|S''\rangle$, and a two-hole triplet state $|T_m\rangle$. (See Appendix B of II for details.) There are further states with three and four holes per cell, but these are higher in energy and will not be considered further. (The effect of these multiple-hole states may be estimated by perturbation theory and shown to be very small.)

The Hamiltonian may now be readily expressed in terms of the cell eigenstates, $|\nu\rangle$, using Hubbard's so-called $X$ operators[45] $X_i^{\nu'\nu}\equiv|i\nu'\rangle\langle i\nu|$,

$$H=\sum_i\sum_\nu E_\nu X_i^{\nu\nu}$$
$$+\sum_{\langle ij\rangle}\sum_{\nu\nu'\mu\mu'}\langle i\nu',j\mu'\,|H_{\rm cc}|i\nu,j\mu\rangle\,X_i^{\nu'\nu}X_j^{\mu'\mu}, \qquad (2.9)$$

where the second sum is over all pairs of sites (but not restricted to nearest neighbors). As pointed out by Hayn *et al.*,[24] the matrix elements $\langle i\nu',j\mu'|H_{\rm cc}|i\nu,j\mu\rangle$ may be computed explicitly by first calculating the cell-independent coefficients in the expansions $d_{x,i\sigma}=\Sigma_{\nu'\nu}\langle\nu'|d_{x,\sigma}|\nu\rangle X_i^{\nu'\nu}$ and $b_{i\sigma}=\Sigma_{\nu'\nu}\langle\nu'|b_\sigma|\nu\rangle X_i^{\nu'\nu}$ and then substituting these expansions into the cell-cell interaction $H_{\rm cc}$ in two-band $d$-$b$ representation, Eqs. (2.4),(2.7),(2.8). We emphasize that the Hamiltonian expressed in this cell basis is entirely equivalent to the Hamiltonian in the $d$-$b$ basis [except that we have omitted now the three- and four-site terms, which would simply have added to Eq. (2.9) terms containing products of three and four Hubbard operators].

Finally in this section, we note that the cell-cell interaction terms fall into two classes. In the first class the occupation numbers of the cell states remain unchanged under the action of $H_{\rm cc}$. They include diagonal matrix elements $\langle i\nu,j\mu|H_{\rm cc}|i\nu,j\mu\rangle=v_{ij}^{\nu\mu}$, which are independent of the spin of any of the states involved, such as $\langle ig_\sigma,jS|H_{\rm cc}|ig_\sigma,jS\rangle\equiv v_{ij}^{gS}$. These may be regarded as effective Coulomb interactions between cells. There are also effective exchange interactions between cells, such as $\langle ig_\sigma,jg_{\bar\sigma}|H_{\rm cc}|ig_{\bar\sigma},jg_\sigma\rangle\equiv j_{ij}^{g}$. The second class involves the transfer of a hole from one cell to another and these terms may be regarded as effective tight-binding hopping terms between cells. Our convention for the corresponding matrix elements is $\langle i\nu',j\mu'|H_{\rm cc}|i\nu,j\mu\rangle\equiv t_{ij}^{\nu'\nu\mu'\mu}$, where the cell state $|\nu'\rangle$ ($|\mu'\rangle$) contains one more (less) hole than $|\nu\rangle$ ($|\mu\rangle$). For example, the matrix element $\langle iS,j0|H_{\rm cc}|ig_\downarrow,jg_\uparrow\rangle\equiv t_{ij}^{Sg0g}$ represents a hole hopping from cell $j$ to cell $i$, for the case where each cell contains one hole in the initial state, whereas $\langle iS,jg_\sigma|H_{\rm cc}|ig_\sigma,jS\rangle\equiv t_{ij}^{SggS}$ represents the exchange of a ZR singlet with a spin.

## III. EFFECTIVE SINGLE-BAND MODEL BY THE CELL METHOD

### A. Form of the effective Hamiltonian

In this section we will describe how the two-band model may be reduced to an effective single-band Hubbard model

and present detailed results on the variation of the effective single-band parameters with the parameters of the underlying $d$-$p$ model (i.e., $t_{pd}$, $t_{pp}$, $\bar{\varepsilon}$, $U_d$, $U_p$, and $V_{pd}$). We will, where possible, give physical reasons for the behavior observed and emphasize any special properties of the effective model for the parameter range appropriate to the cuprates. The parameter range for which the mapping is expected to be valid will also be discussed. This essentially extends our earlier work in which we considered only the mapping to a charge-spin model by the cell method with the approximations $U_d=\infty$ and $U_p=V_{pd}=0$.[14]

The simplest way to construct an effective single-band Hamiltonian from the two-band model described in the previous section is to simply restrict the cell basis set in Eq. (2.9) to the lowest-energy states on each cell, i.e., the "vacuum" state $|0\rangle$, the lowest one-hole state $|g_\sigma\rangle\equiv|\sigma\rangle$, and the lowest two-hole state $|S\rangle$ (the Zhang-Rice singlet). This is equivalent to first-order perturbation theory giving an effective Hamiltonian $H_{\rm eff}=PHP$, where $P$ is the projection operator for all many-cell states in this restricted basis set. Explicitly, $H_{\rm eff}$ is, from Eq. (2.9),

$$
\begin{aligned}
H_{\rm eff}=&(E_g-E_0)\sum_{i\sigma} X_i^{\sigma\sigma}+[2(E_g-E_0)+U_{\rm eff}]\sum_i X_i^{SS}\\
&+\sum_{\langle ij\rangle\sigma}\{[t_{ij}^{g00g}X_i^{\sigma 0}X_j^{0\sigma}+t_{ij}^{SggS}X_i^{S\sigma}X_j^{\sigma S}+t_{ij}^{Sg0g}\lambda_\sigma(X_i^{\sigma 0}X_j^{\bar\sigma S}+X_i^{S\bar\sigma}X_j^{0\sigma})]+[i\leftrightarrow j]\}\\
&+\sum_{\langle ij\rangle}[v_{ij}^{00}X_i^{00}X_j^{00}+v_{ij}^{SS}X_i^{SS}X_j^{SS}+v_{ij}^{0S}(X_i^{00}X_j^{SS}+X_i^{SS}X_j^{00})]\\
&+\sum_{\langle ij\rangle\sigma}[v_{ij}^{0g}(X_i^{00}X_j^{\sigma\sigma}+X_i^{\sigma\sigma}X_j^{00})+v_{ij}^{Sg}(X_i^{SS}X_j^{\sigma\sigma}+X_i^{\sigma\sigma}X_j^{SS})]\\
&+\sum_{\langle ij\rangle\sigma}[v_{ij}^{gg}X_i^{\sigma\sigma}X_j^{\sigma\sigma}+\bar v_{ij}^{gg}X_i^{\sigma\sigma}X_j^{\bar\sigma\bar\sigma}+j_{ij}X_i^{\sigma\bar\sigma}X_j^{\bar\sigma\sigma}],
\end{aligned}
\tag{3.1}
$$

where $U_{\rm eff}\equiv E_S-2E_g+E_0$, $\lambda_\uparrow=-\lambda_\downarrow=1$, and $\langle ij\rangle$ denotes a pair of cells (not necessarily nearest neighbors). Note that, as implied by the notation, the $v$ matrix elements are independent of spin when one of the two cells is either unoccupied or doubly occupied with holes, but depend on whether the spins are parallel or antiparallel when both cells are singly occupied. As we show later, this spin dependence comes entirely from the $U_p$ term in the original Hamiltonian (2.1). With the help of some Hubbard-operator identities[14] and exploiting rotational invariance, we can, quite generally, make this spin dependence explicit and rewrite the last summation in (3.1) in the form

$$
\sum_{\langle ij\rangle}[v_{ij}^{gg}X_i^{gg}X_j^{gg}+J_{ij}(\mathbf{S}_i\cdot\mathbf{S}_j-\tfrac{1}{4}X_i^{gg}X_j^{gg})], \tag{3.2}
$$

where $X^{gg}\equiv\Sigma_\sigma X^{\sigma\sigma}$, the projector onto the singly occupied cell subspace, and $J_{ij}=2(v_{ij}^{gg}-\bar v_{ij}^{gg})=2j_{ij}$. We have chosen the usual convention of including the term $-\frac{1}{4}\Sigma_{\langle ij\rangle}J_{ij}X_i^{gg}X_j^{gg}$ with the spin part rather than absorbing it in the first term in (3.2). This ensures that the spin part makes no contribution for purely ferromagnetic states.

Comparing (3.1) with the expression one would obtain from the usual single-band Hubbard model[46] when expressed in terms of $X$ operators, one sees that there is a direct correspondence for both the single-cell terms and the two-cell hopping terms. The only essential difference is the electron-hole asymmetry in the hopping terms of (3.1). The extra $v$ (effective Coulomb) terms and the $j$ (effective exchange) term in (3.1) do not appear in the usual Hubbard model. Similar terms do, however, occur in a more general single-band Hubbard model (and were indeed considered by Hubbard). They would give rise to the same forms of interactions present in (3.1), as can be seen explicitly by adding the Coulomb and exchange terms $\Sigma_{\langle ij\rangle}V_{ij}n_in_j+\Sigma_{ij\sigma}J_{ij}c_{i\sigma}^\dagger c_{i\bar\sigma}\bar c_{j\bar\sigma}^\dagger c_{j\sigma}$ to the usual Hubbard model and expressing the result in terms of $X$ operators. Thus $H_{\rm eff}$ given in this "first-order" approximation has exactly the form expected from a single-band Hubbard model, apart from some asymmetry in the effective parameters.

### B. Validity of the effective single-band model

We now discuss the validity and possible breakdown of the effective single-band form given in Eq. (3.1). As with any first-order perturbation approximation, it is reasonably accurate provided that the base states neglected have sufficiently high energies. This is not the case here. However, for a wide range of parameters the base states omitted are sufficiently high in energy that they may be accounted for by perturbation theory or, equivalently, by a Schrieffer-Wolff transformation. Such perturbation corrections have two effects. They renormalize the effective parameters in (3.1) and they give rise to new terms (such as spin-flip scattering terms). In this section we shall include renormalization effects to second order in perturbation theory, deferring a brief discussion of the most important new terms until Sec. IV. In order that a second-order perturbative treatment be reasonable the corresponding expansion parameters must be small. In our case the critical expansion parameters are of the form

$|t/\Delta E|$ where $t$ is a matrix element corresponding to a transition from a state in the ''model subspace'' to states in which one or more cells are in higher-energy excited cell states, and $\Delta E$ is the (unperturbed) energy to make this transition.

In order to understand the dependence of the expansion parameters $|t/\Delta E|$ (and also of the hopping parameters occurring in the effective single-band model; see next section) on the parameters of the underlying $d$-$p$ model, it is helpful to write down explicitly the various contributions to the effective hopping parameters. Not surprisingly, the main contribution comes from the bare $pd$ and $pp$ hopping:

$$t_{\mathrm{hop},ij}^{\nu'\nu\mu'\mu} = -2t_{pd}\mu_{ij}\sum_{\sigma}\ [\langle\nu'|d_{x,\sigma}^{\dagger}|\nu\rangle\langle\mu'|b_{\sigma}|\mu\rangle + \langle\nu'|b_{\sigma}^{\dagger}|\nu\rangle\langle\mu'|d_{x,\sigma}|\mu\rangle] - 2t_{pp}\nu_{ij}\sum_{\sigma}\ \langle\nu'|b_{\sigma}^{\dagger}|\nu\rangle\langle\mu'|b_{\sigma}|\mu\rangle, \tag{3.3}$$

as obtained directly from (2.4) by substituting the Hubbard-operator expansion for $d_{x,i\sigma}$ and $b_{i\sigma}$. Also the Coulomb interactions involving oxygen holes contribute, in particular to nearest-neighbor hopping, because each oxygen, being in a position bridging two cells, contributes to the cell states of both. The contribution made by $V_{pd}$ is, from Eq. (2.7),

$$t_{pd,ij}^{\nu'\nu\mu'\mu} = V_{pd}\phi_{iij}\sum_{\sigma}\ [\langle\nu'|n^{(d)}b_{\sigma}^{\dagger}|\nu\rangle\langle\mu'|b_{\sigma}|\mu\rangle + \langle\nu'|b_{\sigma}^{\dagger}|\nu\rangle\langle\mu'|n^{(d)}b_{\sigma}|\mu\rangle - 2n_g^{(d)}\langle\nu'|b_{\sigma}^{\dagger}|\nu\rangle\langle\mu'|b_{\sigma}|\mu\rangle], \tag{3.4}$$

where $n_g^{(d)} \equiv \langle g_\sigma|n^{(d)}|g_\sigma\rangle$. We recall that the first two terms correspond to ''direct'' hopping from cell $i$ to cell $j$, while the last, ''indirect,'' term arises from the hops via all *other* cells $l$, and the choice $\bar{n}^{(d)} = n_g^{(d)}$ assumes that those cells all carry a one-hole cell state $|g_\sigma\rangle$. Obviously, therefore, Eq. (3.4) embodies a specific assumption about the ''background'' in which the hop is taking place. Such an assumption is inevitable because of the occurrence of what are formally three-cell terms [compare Eq. (2.5)], so that strictly speaking any hopping matrix element induced by $V_{pd}$ depends on the occupation of *all* cells, not just of the cells between which the hop actually occurs. In the low doping regime the choice implied by (3.4) seems most appropriate, since it takes the half-filled band insulator as reference system. Then only deviations from that uniform one-hole-per-cell background, such as the presence of a nearby ZR singlet, give rise to ''true'' three-cell terms in the effective Hamiltonian [compare Eq. (2.7)] which we argued to be small and further ignored. Note that omitting the ''indirect'' term in (3.4) on the formal ground that it is a three-cell term would actually amount to taking the fully electron-doped system as reference and must lead to larger three-cell corrections near half-filling. Similarly, the $U_p$ contribution is, using Eq. (2.8),

$$t_{p,ij}^{\nu'\nu\mu'\mu} = U_p\psi_{iiij}\sum_{\sigma}\ [\langle\nu'|n_{\bar{\sigma}}^{(b)}b_{\sigma}^{\dagger}|\nu\rangle\langle\mu'|b_{\sigma}|\mu\rangle + \langle\nu'|b_{\sigma}^{\dagger}|\nu\rangle\langle\mu'|n_{\bar{\sigma}}^{(b)}b_{\sigma}|\mu\rangle - n_g^{(b)}\langle\nu'|b_{\sigma}^{\dagger}|\nu\rangle\langle\mu'|b_{\sigma}|\mu\rangle]. \tag{3.5}$$

Again, the first two terms correspond to direct hopping from cell $i$ to cell $j$, while the last, indirect, term arises from the hops via all *other* cells $l$. Here we have set $\bar{n}_{\uparrow}^{(b)} = \bar{n}_{\downarrow}^{(b)} = \frac{1}{2}n_g^{(b)}$, equivalent to the assumption that all those cells carry a $|g_\sigma\rangle$ cell state with equal probability for the spin to be up or down. This choice of a ''paramagnetic'' background, although probably not realized at half-filling, seems to be the only obvious way to keep (3.5) spin independent, i.e., to put all spin dependence in the ''true'' three-cell terms (which we further ignore).

Equations (3.3), (3.4), and (3.5) clearly show that the magnitude of any hopping matrix element, and in particular the relative contributions made by $t_{pd}$ and $t_{pp}$, depends critically on the precise composition of the cell states involved. More specifically, there will be interference between contributions coming from the various component basis states in each cell state. One further observes from Eqs. (3.4) and (3.5) that for the direct terms in $t_{pd,ij}^{\nu'\nu\mu'\mu}$ and $t_{p,ij}^{\nu'\nu\mu'\mu}$ to be nonzero, at least one of the cell states must be a two-hole state, while there is no such restriction for the indirect terms. One thus expects the contributions from $V_{pd}$ and $U_p$ to hopping parameters for two-hole states to be significantly smaller than to hopping involving only zero-hole and one-hole states, because of partial cancellation in the former case. As regards the Wannier transformation coefficients, those relevant for nearest-neighbor hopping are $\mu_{01} = -0.1401$, $\nu_{01} = -0.2732$, $\phi_{001} = -0.1342$, $\psi_{0001} = -0.0303$, those for next-nearest-neighbor hopping $\mu_{02} = -0.0235$, $\nu_{02} = +0.1221$, $\phi_{002} = -0.0225$, $\psi_{0002} = -0.0052$. This shows that the hopping contributions coming from $V_{pd}$ and (in particular) $U_p$ will be generally smaller than those from $t_{pd}$ and $t_{pp}$. The relative signs imply that the Coulomb terms oppose the effect of $pd$ hopping and therefore reduce the magnitude of the hopping matrix elements when the direct terms are larger than the indirect term and vice versa. Note, however, that $V_{pd}$ and $U_p$ also affect the magnitude of (3.3) by modifying the wave functions of the two-hole cell states.

An examination of the eigenspectrum of the single-cell Hamiltonian, Eq. (2.9), shows that, over the whole parameter range of interest, there is one ''excited'' cell state which is closer to the states in the ground manifold than the remaining excited states. This is the two-hole triplet state, the importance of which was first pointed out by Emery and Reiter.[34] We shall refer to it as the Emery-Reiter (ER) triplet. The important perturbation expansion parameters involving these triplet cell states are $|t^{Tg0g}/(E_T - 2E_g + E_0)|$ and $|t^{TggS}/(E_T - E_S)|$, where $t^{Tg0g} = \langle T_0, 0|H_{\mathrm{cc}}|g_\sigma, g_{\bar{\sigma}}\rangle$ and $t^{TggS} = \lambda_{\bar{\sigma}}\langle T_0, g_\sigma|H_{\mathrm{cc}}|g_\sigma, S\rangle$. Plots of these ratios for various parameters are shown in Figs. 1 and 2. (Here, as in all figures to follow, all quantities are dimensionless, energies being plotted in units of $t_{pd}$.) We see that over the whole parameter range, which includes both the insulating and metallic regimes in the half-filled band case, these ratios remain quite small, hardly exceeding 0.1. Thus we expect second-order

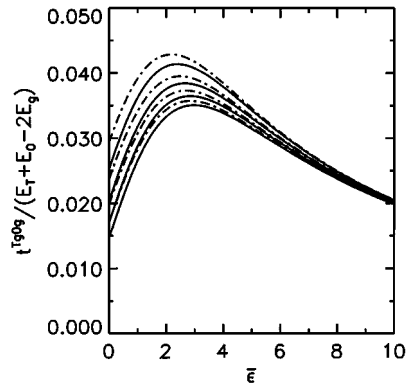


FIG. 1. $|t^{Tg0g}/(E_T-2E_g+E_0)|$ vs $\bar{\varepsilon}$ for $U_p=0$ (solid line) and $U_p=3$ (dot-dashed line) and $V_{pd}=0$, 1, 2, 3 (from top to bottom). Note that $\bar{\varepsilon}$ is in units of $t_{pd}$, as all quantities with the dimension of energy will be in all figures to follow.

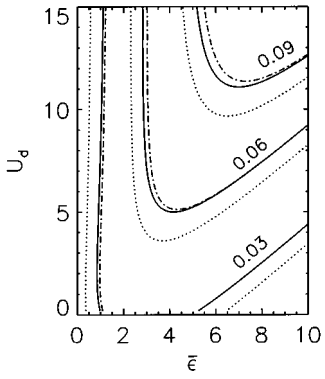


FIG. 2. Contour plots of $|t^{TggS}/(E_T-E_S)|$ vs $U_d$ and $\bar{\varepsilon}$ for $V_{pd}=U_p=0$ (dotted line), $V_{pd}=1$, $U_p=0$ (dot-dashed line), and $V_{pd}=1$, $U_p=3$ (solid line).

perturbation theory to be reasonably accurate. The present results confirm previous investigations for $V_{pd}=U_p=0$,[24,25] and in addition show that over the parameter range of interest the net effect of the Coulomb terms $U_p$ and $V_{pd}$ actually is to *decrease* these ratios, thereby improving the convergence. As pointed out above, this is due mainly to a reduction of the hopping matrix elements, in agreement with the expectation that Coulomb repulsion suppresses kinetic energy. Note, however, that this trend must eventually reverse since we can make the hopping matrix elements arbitrarily large by suitably increasing the Coulomb parameters $U_p$ and $V_{pd}$ [compare Eqs. (3.4) and (3.5)]. This would indeed signal a breakdown of the cell method. It is fortunate, and rather surprising *a priori*, that this breakdown does not occur for any reasonable values of the Coulomb parameters. We give a simple explanation of this below when we discuss the first-order contribution to superexchange.

In Fig. 1 the variation of $|t^{Tg0g}/(E_T-2E_g+E_0)|$ with $\bar{\varepsilon}$ is plotted for different values of $V_{pd}$ and $U_p$. The curves pass through a maximum since $E_T-2E_g+E_0$ decreases initially as $\bar{\varepsilon}$ is increased from zero (because $E_g$ increases due to reduced $d$-$p$ hybridization), but must eventually increase for large $\bar{\varepsilon}$ since $E_T=\bar{\varepsilon}+V_{db}$. The suppression of the ratio when $V_{pd}$ is increased is due both to the reduction of the hopping parameter (which always has a $V_{pd}$ contribution of opposite sign to that due to $t_{pd}$ and $t_{pp}$) and to the increased triplet energy. The small opposite effect of $U_p$ is caused by the indirect contribution to the hopping parameter, the direct term being zero for the triplet [compare Eq. (3.5)]. The ratio is, of course, unaffected by $U_d$ since the triplet state has no component with two holes on copper.

The contour plots in Fig. 2 are similar, showing again a rather strong suppression of $|t^{TggS}/(E_T-E_S)|$ with the Coulomb parameter $V_{pd}$, with a somewhat weaker dependence on $U_p$. The ratio remains small when either $U_d$ and/or $\bar{\varepsilon}$ are small, because the ZR singlet can then lower its energy by hybridization with $|d_{x,\uparrow}d_{x,\downarrow}\rangle$ and/or $|b_\uparrow b_\downarrow\rangle$, making $E_T-E_S$ large. Only when *both* $U_d$ and $\bar{\varepsilon}$ are large is the energy lowering of the ZR singlet small and the ratio becomes large. (Note that in the limit $U_d,\varepsilon\to\infty$, while $U_d>\varepsilon$, the ZR singlet and the ER triplet become degenerate.) The large effect of $V_{pd}$ is again due to the suppression of the hopping matrix element ($t^{TggS}$) and the increase in triplet energy relative to the singlet (since the latter has a component in the state $|b_\uparrow b_\downarrow\rangle$ which does not make a $V_{pd}$ contribution to the energy).

In addition to the ER triplet, there is one further excited cell state which could influence the convergence of the perturbation expansion to an effective single-band model, namely, the excited state of a singly occupied cell, $|e_\sigma\rangle$. Propagation of this state leads to a transport of energy but not of charge and in this sense it may be regarded as a Frenkel exciton. Compared to the one-hole ground state $|g_\sigma\rangle$ the excited state $|e_\sigma\rangle$ is an *intracell* kind of $d\to p$ charge-transfer excitation, the corresponding *intercell* excitation being the simultaneous creation of a "free" ($d$-like) electron $|0\rangle$ in the upper Hubbard band and a "free" ($p$-like) Zhang-Rice hole $|S\rangle$ in the lower Hubbard band. Actually, the Frenkel exciton is "created" when neighboring cells containing a ZR singlet $|S\rangle$ and an electron state $|0\rangle$ are transformed to a one-hole ground state $|g_\sigma\rangle$ on one cell and a one-hole excited state $|e_{\bar{\sigma}}\rangle$ on the other by a hole hopping process. The transfer matrix element for this process is $t^{e0gS}\equiv\langle e_{\bar{\sigma}},g_\sigma|H_{\rm cc}|0,S\rangle$ and hence the relevant expansion parameter is $|t^{e0gS}/(E_g+E_e-E_S-E_0)|$. Contour plots of this quantity with respect to $U_d$ and $\bar{\varepsilon}$ are shown in Fig. 3 for various $U_p$ and $V_{pd}$. We see that the sensitivity to $U_p$ is quite small, but the effect of $V_{pd}$ is significant. Near the top of the ZSA plot (where $U_d$ and $\bar{\varepsilon}$ are relatively large) the expansion

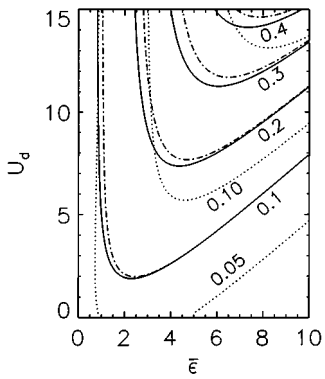


FIG. 3. Contour plots of $|t^{e0gS}/(E_g+E_e-E_S-E_0)|$ vs $U_d$ and $\bar{\varepsilon}$ for $V_{pd}=U_p=0$ (dotted line), $V_{pd}=1$, $U_p=0$ (dot-dashed line), and $V_{pd}=1$, $U_p=3$ (solid line).

parameter can be quite appreciable. The main reason is the decrease in the energy denominator, since when $\bar{\varepsilon}$ is very large the $d$-$p$ hybridization is small, and hence $E_g \to \varepsilon_d$, $E_e \to \varepsilon_p$, and $E_S \to \varepsilon_d + \varepsilon_p$, provided $U_d$ is also large. The regime where this occurs is shifted to significantly smaller values of $\bar{\varepsilon}$ and $U_d$ when $V_{pd}$ is increased. Indeed, for $V_{pd}=2$ the ratio even diverges in the range covered in Fig. 3. The reason is that $V_{pd}$ raises the energy of the Zhang-Rice singlet but leaves the energy of $|e_\sigma\rangle$ (being a single-hole state) unaffected. Thus the charge-transfer exciton ($g \to e$), which for small $V_{pd}$ is *antibound* with respect to the interband excitation ($gg \to S0$) because of the large energy gain from hybridization by the free ZR singlet, becomes degenerate with it for sufficiently large $V_{pd}$ (and finally falls below it). So when the copper-oxygen Coulomb interaction is strong, the presence of the charge-transfer exciton state $|e_\sigma\rangle$ can no longer be ignored if also $U_d$ and $\bar{\varepsilon}$ are fairly large, and formally this invalidates the description of the charge-transfer system by an effective single-band model. However, under these conditions $U_{\rm eff}$ is so large (compare Fig. 4) that *all* charge-transfer excitations are strongly suppressed; i.e., for hole doping both $|0\rangle$ and $|e_\sigma\rangle$ become irrelevant, for electron doping both $|S\rangle$ and $|e_\sigma\rangle$ can be ignored, and one can make a further reduction to a charge-spin model (see Sec. IV). Note that for the parameter range actually of interest for the cuprates the validity of the perturbation expansion is not an issue. Nevertheless, the charge-transfer exciton can give rise to appreciable perturbation corrections which are at least comparable with those due to the Emery-Reiter triplet.

### C. Effective Hubbard-$U$ and hopping terms

If we ignore the the ''static'' interactions between neighboring cells [i.e., the $v$ interactions in Eq. (3.1)] and switch off the hopping between cells (the $t$ terms), then the energy required to take a hole from a singly occupied cell and place it on another singly occupied cell with opposite spin is $E_S - 2E_g + E_0 \equiv U_{\rm eff}$, as shown in Eq. (3.1). By analogy with the usual single-band Hubbard model, we regard this quantity as an effective Coulomb repulsion between two holes on the same cell. (We show later that this definition is not appropriate when the $v$ terms are finite and we must correct $U_{\rm eff}$. This correction is relatively small over the parameter regime of interest though not negligible. See Sec. III E.) In Fig. 4 we show contour plots of $U_{\rm eff}$ of the type considered by Zaanen, Sawatzky, and Allen (ZSA),[33] who used them for characterizing Mott insulators and charge-transfer insulators. These show clearly the expected behavior in the charge-transfer regime ($\bar{\varepsilon} \ll U_d$), and Mott-Hubbard regime ($\bar{\varepsilon} \gg U_d$). In the latter $U_{\rm eff} \to U_d$ and becomes independent of $\bar{\varepsilon}$, $U_p$, and $V_{pd}$, whereas in the extreme CT regime $U_d$ becomes irrelevant though both $U_p$ and $V_{pd}$ increase $U_{\rm eff}$ significantly. For the parameter regime of physical interest, in which the corrections to the effective single-band picture may be accounted for perturbatively, $U_{\rm eff}$ spans a broad range of values ($\approx 2-15$ eV). For the special case of an ''effective'' half-filled band (i.e., an average of one hole per cell) this includes both metallic and insulating phases. The interesting region of the metal-insulator transition will be discussed further in Sec. III F. For the ''standard'' set of cuprate parameters we find for $U_{\rm eff}$ a value of 2.5 in units of $t_{pd}$, amounting to $\approx$ 3.2 eV.

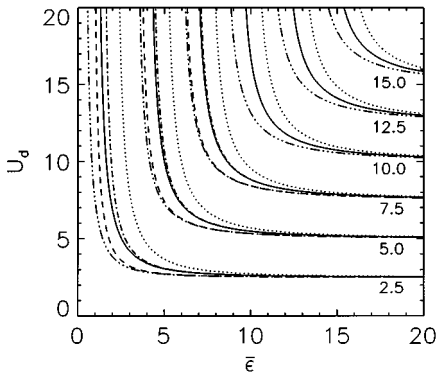


FIG. 4. Contour plots of $U_{\rm eff}$ vs $U_d$ and $\bar{\varepsilon}$ for $V_{pd}=U_p=0$ (dotted line), $V_{pd}=1$, $U_p=0$ (dot-dashed line), $V_{pd}=1$, $U_p=3$ (solid line), $V_{pd}=2$, $U_p=0$ (dashed line), and $V_{pd}=2$, $U_p=3$ (multidot-dashed line).

Let us now consider the various *nearest-neighbor* effective hopping matrix elements in the single-band Hamiltonian (3.1). These are labeled $t^{hh} \equiv t^{SggS}$, $t^{ee} \equiv t^{g00g}$, and $t^{eh} \equiv t^{g0gS}$. This suggestive notation signifies electron and hole hopping *relative to cell states containing one hole (spin)* in which $|S\rangle$ represents a hole, $|0\rangle$ represents an electron, and $|\sigma\rangle \equiv |g_\sigma\rangle$ represents a spin. Thus, $t^{hh}$ is the matrix element for a hopping process in which a Zhang-Rice singlet changes places with a spin on a neighboring cell, which is equivalent to a hole hop. Similarly $t^{ee}$ represents an electron hop and $t^{eh}$ represents the creation of an electron-hole pair from two spins, or vice versa ($|\sigma,\bar{\sigma}\rangle \leftrightarrow |0,S\rangle$).[47] In Fig. 5 we show the variation of $t^{hh}$, $t^{ee}$, and $t^{eh}$ with $\bar{\varepsilon}$ for various $U_d$ and for $t_{pp}=0$ and 0.5. (In these graphs we set $U_p=V_{pd}=0$.) The purpose of these plots is to show the magnitude and asymmetry of the three hopping matrix elements and their dependence on copper Coulomb repulsion $U_d$ and oxygen bandwidth $t_{pp}$. In all cases (except for $\bar{\varepsilon} \gg U_d$ when hopping via $t_{pd}$ dominates) the effect of finite oxygen bandwidth is to increase the effective hopping considerably, as recognized in earlier estimates for the cuprates.[10,11,13,14,16] This is expected since $t_{pp}$ provides a new channel for hopping between cells. We see further that, in general, there can be a significant asymmetry except for small $U_d$ [Fig. 5(c)].

Although the dependence on the parameters via the matrix elements is quite complicated [see Eq. (3.3)], for finite $t_{pp}$ the electron hopping parameter $t^{ee}$ is in general smaller than the hole hopping parameter $t^{hh}$ due to the fact that the probability for a hole to be on oxygen is greater for a Zhang-Rice singlet than for the doublet state ($|g_\sigma\rangle$) (with the exception of $U_d=\infty$). Note that in the parameter region corresponding to the cuprates [Fig. 5(b) with $\bar{\varepsilon} \approx 2$] the asymmetry is quite large with $t^{hh} > t^{eh} > t^{ee}$. However, this situation changes when we consider the further Coulomb terms $U_p$ and $V_{pd}$. This is shown in Fig. 6 where we plot $t^{hh}$ and $t^{ee}$ in the same way but include the effects of $U_p$ and $V_{pd}$ (with $t_{pp}=0.5$ and for the typical case $U_d=7$, the behavior being very similar for other values of $U_d$). The effect of these Coulomb terms is as expected from the considerations following Eqs. (3.4) and

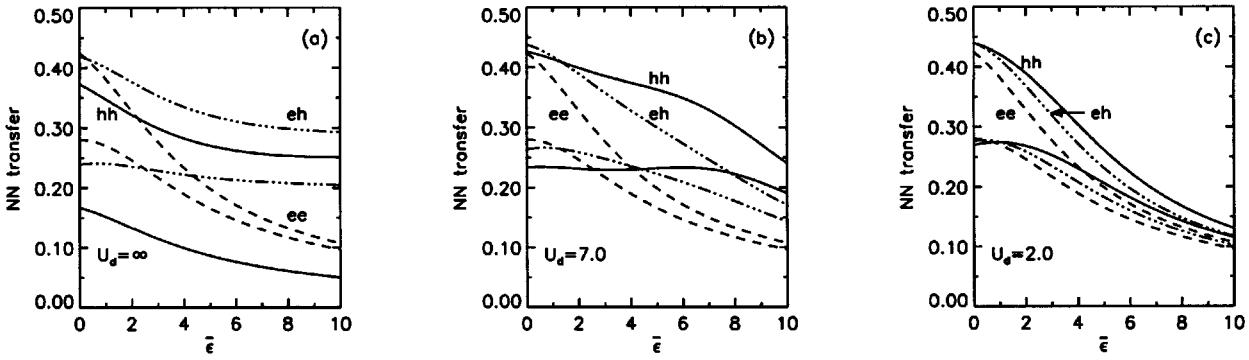


FIG. 5. Nearest-neighbor hopping for electrons (dashed lines), for holes (solid lines), and for electron-hole transitions (multidot-dashed lines) showing the effect of finite oxygen bandwidth [$t_{pp}=0.5$ for upper curves (marked $ee$, $hh$, and $eh$) and $t_{pp}=0$ for lower curves]: (a) $U_d=\infty$, (b) $U_d=7$, (c) $U_d=2$.

(3.5). Hole hopping is little affected, the direct and indirect terms coming from $V_{pd}$ (although each about 0.1 in magnitude for $V_{pd}=1$) nearly canceling each other. Moreover, at small $\bar{\varepsilon}$ where the $|b_\uparrow b_\downarrow\rangle$ component in $|S\rangle$ becomes sizable and the indirect $V_{pd}$ term wins, the resulting small increase in $t^{hh}$ due to $V_{pd}$ is partially canceled by the contribution from $U_p$ for which the direct term is always the larger. By contrast, electron hopping is enhanced, in particular by $V_{pd}$ and especially at small $\bar{\varepsilon}$ where [compare Eq. (3.4)] $n_g^{(d)}=\cos^2\theta$ and the squared matrix element, which equals $n_g^{(b)}=\sin^2\theta$, become equally large. The interband matrix element $t^{eh}$ is enhanced as well. This enhancement can be quite appreciable in the expected parameter range of the cuprates. For example, with $U_p\approx 4$ eV and $V_{pd}\approx 1.3$ eV, $t^{ee}$ is increased from $\approx 0.42$ eV (when $U_p=V_{pd}=0$) to $\approx 0.50$ eV, and $t^{eh}$ from $\approx 0.51$ eV to $\approx 0.56$ eV, while $t^{hh}$ remains virtually unchanged at $\approx 0.51$ eV. It is clear from Figs. 5 and 6 that the almost exact equality of $t^{hh}$ and $t^{ee}$, i.e., the *nearly perfect electron-hole symmetry* for cuprate parameters, which has also been found in cluster calculations,[10–12] is *purely coincidental*. The present values, although a little larger, are in good agreement with that work [$t^{hh}=t^{ee}=0.40$ eV (Ref. 10); $t^{hh}=0.41$ eV, $t^{ee}=0.44$ eV (Ref. 11); $t^{hh}=0.22$ eV, $t^{ee}=0.30$ eV (Ref. 12)].

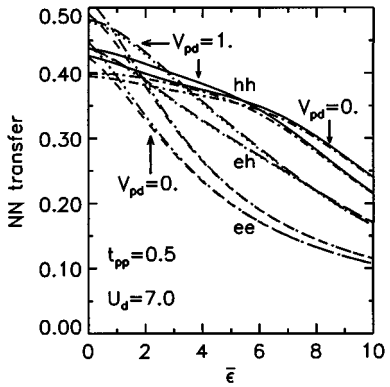


FIG. 6. Nearest-neighbor hopping for electrons (dashed lines for $U_p=0$ and multidot-dashed lines for $U_p=3$), for holes (solid lines for $U_p=0$ and dot-dashed lines for $U_p=3$), and for electron-hole transitions (long-dashed lines for $U_p=0$ and dotted lines for $U_p=3$), for $V_{pd}=0$ and $V_{pd}=1$ as indicated, for $U_d=7$ and $t_{pp}=0.5$.

In Fig. 7 we consider *next-nearest-neighbor* hopping ($t'$) for both holes and electrons. Here we again see a significant asymmetry and, in particular, for the parameters corresponding to the cuprates the magnitude of these effective hopping parameters is much smaller for electrons than for holes. As comparison between Figs. 7(a) and 7(b) immediately shows, this large asymmetry is caused by the rather different effect of $t_{pp}$ on $t'^{hh}$ and $t'^{ee}$. This is mainly due to the fact that for next-nearest-neighbor hopping the first-order contribution [Eq. (3.3)] from $t_{pp}$ opposes that from $t_{pd}$, because the relevant coefficients $\nu_{02}=+0.1221$ and

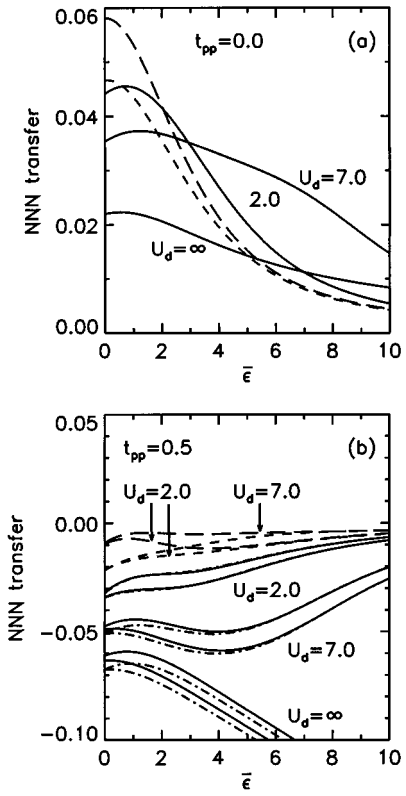


FIG. 7. Next-nearest-neighbor hopping for (a) $t_{pp}=0$ and (b) $t_{pp}=0.5$, showing the effect of finite oxygen bandwidth. Electrons: dashed lines for $V_{pd}=U_p=0$, long-dashed lines for $V_{pd}=1$ and $U_p=0$. Holes: solid lines for $U_p=0$ and dot-dashed lines [in (b) only] for $U_p=3$. In (b) lower line for $V_{pd}=0$ and upper line for $V_{pd}=1$, for each value of $U_d$.

$\mu_{02}=-0.0235$ have opposite sign due to the phasing of the Wannier orbitals. Since the coefficient for $t_{pp}$ is much larger because it involves a direct hopping process, $t_{pp}$ makes the dominant contribution to next-nearest-neighbor *hole* hopping as long as $\bar{\varepsilon} \lesssim U_d$ (so that the ZR singlet is predominantly $b$ like, with the $db$-singlet component larger than the $|d_{x,\uparrow} d_{x,\downarrow}\rangle$ component), and consequently $t'^{hh}_{\rm hop}<0$. By contrast, $t_{pd}$ dominates *electron* hopping as long as $\bar{\varepsilon} \gtrsim 1$ (so that the one-hole state is predominantly $d$ like, i.e., $\cos\theta > \sin\theta$ in $|g_\sigma\rangle = \cos\theta |d_{x,\sigma}\rangle + \sin\theta |b_\sigma\rangle$, and $pd$ hopping $\propto \sin\theta\cos\theta$ is larger than $pp$ hopping $\propto \sin^2\theta$), and $t'^{ee}_{\rm hop}>0$. Note further that for electrons $V_{pd}$ always enhances $pd$ hopping and therefore supports the tendency for $t'^{ee}$ to remain positive.

The results shown in Figs. 6 and 7 not only include the first-order contributions to the effective hopping parameters, i.e., from Eqs. (3.3), (3.4), and (3.5), but also second-order corrections, such as considered in Ref. 14, arising from intermediate states that contain an excited cell state. By far the most important contributions come from the ER triplet, which generates for example a correction to hole (i.e., ZR singlet) hopping via the process $|S,g,g\rangle \rightarrow |g,T,g\rangle \rightarrow |g,g,S\rangle$; i.e. the ZR singlet on cell 1 exchanges with a spin ($|g_\sigma\rangle$) on cell 3 via an intermediate state involving an ER triplet on cell 2. Similarly the excited singlets $|S'\rangle$ and $|S''\rangle$ contribute via the process $|S,g,g\rangle \rightarrow |g,S',g\rangle \rightarrow |g,g,S\rangle$. For the corrections to electron hopping one has to consider processes like $|0,g,g\rangle \rightarrow |0,T,0\rangle \rightarrow |g,g,0\rangle$, etc. As explained in Ref. 14 these second-order processes actually lead to three-cell terms: their contribution to hopping from cell $i$ to cell $j$ depends on the orientation of the spin on the intervening cell $l$ and may also involve a spin flip. (In addition, we require that cell $l$ carry a spin, and not a zero-hole state or a ZR singlet, in which case different processes would contribute, such as $|S,S,g_\sigma\rangle \rightarrow |g_\sigma, \bar{f}_{\bar{\sigma}}, g_\sigma\rangle \rightarrow |g_\sigma, S, S\rangle$, where $\bar{f}_\sigma$ is a three-hole cell state.) One therefore faces here a similar problem as with the hopping terms generated by the Coulomb interactions, namely, what to include in the hopping terms proper, and what to consider as "true" three-cell terms. In order to have consistency with the choice made above, we again assume a reference paramagnetic "background"; i.e. all other cells carry a one-hole state with equal probability for spin up or spin down. We thus include the mean of spin-parallel and spin-antiparallel non-spin-flip terms in the second-order renormalization of the hopping parameters, thus designating their difference as well as the spin-flip terms as true three-cell terms.

For *nearest*-neighbor hopping ($t^{hh}$, $t^{ee}$, $t^{eh}$) the ensuing modification is negligibly small ($\lesssim 2\%$), because one of the virtual hops in the second-order process is itself a (first-order) next-nearest-neighbor (or more distant) hop. However, for *next-nearest*-neighbor hopping the correction can be comparable with the first-order contribution. The explanation for this large effect is, first, that the two virtual hops can now be both nearest-neighbor hops, and second, that the first-order results are fairly small themselves due to the cancellations discussed above. The fact that first- and second-order contributions are of similar size does not imply that the perturbation expansion is poorly convergent, but is merely a consequence of the fact that first- and second-order contributions arise from physically distinct processes. Higher-order corrections are much smaller, as may be seen from the plots of the relevant expansion parameters in Figs. 1 and 2.

An interesting consequence is that while the second-order corrections make the hole hopping parameter $t'^{hh}$ simply more negative, they switch the sign of the electron hopping parameter $t'^{ee}$ from positive to (just) negative. For example, for the "standard" cuprate parameter set we find $t'^{hh}=-0.06$ eV, $t'^{ee}=-0.01$ eV. Comparing with the earlier work on clusters [$t'^{hh}=-0.17$ eV, $t'^{ee}=-0.10$ eV (Ref. 10); $t'^{hh}=-0.06$ eV, $t'^{ee}=-0.07$ eV (Ref. 11); $t'^{hh}=-0.12$ eV, $t'^{ee}=-0.06$ eV (Ref. 12)] we see that there is some discrepancy here, in particular for the electron hopping parameter. We believe that the present cell-method values are more accurate, since, as pointed out before,[14,48] the cluster calculations either miss or underestimate (in clusters containing two copper ions[10,12] or five copper ions,[11] respectively) the contribution from $pd$ hopping, which always involves physically a hopping process via a third copper atom.[49] They therefore tend to give estimates for the effective next-nearest-neighbor hopping that are too negative, in particular for $t'^{ee}$, where the $t_{pd}$ contribution actually dominates, as argued above. We stress that the very small value for $t'^{ee}$, much smaller than that for $t'^{hh}$, is a very robust result of our calculations, which is also rather insensitive to the precise way in which the second-order corrections are handled. The significance of these results for next-nearest-neighbor hopping will be discussed in Sec. V.

### D. Spin-dependent terms

We now consider the Coulomb and exchange terms in the effective Hamiltonian, i.e., the $v$ terms and the $j$ term in Eq. (3.1), starting with the spin-dependent terms, which are potentially important for the low-energy states when the effective single band is close to being half full. Indeed, exactly at half-filling (i.e., when the number of holes equals the number of sites), there is a $2^N$-fold degenerate set of noninteracting cell states with one hole (spin) on each cell which are lowest in energy, being separated from excited states by a gap of order $U_{\rm eff}$. Within this degenerate manifold all interactions in (3.1) are zero or constant, apart from some contributions to the last two terms in (3.1) which depend on spin (and thus split the degenerate manifold.) Thus, when $U_{\rm eff}$ is large we expect such spin-dependent interactions to become important.

It is clear that, in first order, they arise only from the $U_p$ term in the original $d$-$p$ model, i.e., from the interaction

$$H_p = U_p \sum_i \left(p^\dagger_{x,i\uparrow} p_{x,i\uparrow} p^\dagger_{x,i\downarrow} p_{x,i\downarrow} + p^\dagger_{y,i\uparrow} p_{y,i\uparrow} p^\dagger_{y,i\downarrow} p_{y,i\downarrow}\right). \tag{3.6}$$

Furthermore, it is only the matrix elements of this operator between two cell states in which both cells are singly occupied with holes (spins) that are spin dependent, i.e., $\langle i\uparrow, j\uparrow | H_p | i\uparrow, j\uparrow\rangle = 0$, whereas $\langle i\uparrow, j\downarrow | H_p | i\uparrow, j\downarrow\rangle = -\langle i\uparrow, j\downarrow | H_p | i\downarrow, j\uparrow\rangle \neq 0$, etc., for any two cells located at $i$ and $j$. These matrix elements fall off rapidly with distance, as do other Coulomb matrix elements, and in what follows we shall restrict ourselves to only nearest-neighbor cell interactions. Substituting these results into the last term in Eq. (3.2) yields directly the sum of all spin-dependent terms,

$$H_{\rm spin}^{(p)}=J_p\sum_{\langle ij\rangle}(\mathbf{S}_i\cdot\mathbf{S}_j-\tfrac{1}{4}X_i^{gg}X_j^{gg}), \tag{3.7}$$

where $J_p=-2\langle\uparrow,\downarrow|H_p|\uparrow,\downarrow\rangle<0$, and the sum is restricted to nearest-neighbor pairs. Hence the direct spin-dependent terms in first order give rise to a Heisenberg interaction with a ferromagnetic exchange. This is, of course, due directly to the Pauli principle and the oxygen Coulomb repulsion: when the spins are antiparallel there is always some probability in the ground state that an oxygen site will be doubly occupied and this pushes up the energy by a factor proportional to $U_p$. Now $U_p$ can be quite large ($\approx 3-6$ eV) and we might thus expect *a priori* that this would render a cell-perturbation expansion poorly convergent or even divergent. This, however, is not the case as can be seen from an examination of the nearest-neighbor two-cell matrix element $\langle\uparrow,\downarrow|H_p|\uparrow,\downarrow\rangle$. Expanding this in terms of the $d_x$ and $b$ orbitals for the two cells using $|\sigma\rangle\equiv|g_\sigma\rangle=\cos\theta\,|d_{x,\sigma}\rangle+\sin\theta|b_\sigma\rangle$ we get

$$\langle\uparrow,\downarrow|H_p|\uparrow,\downarrow\rangle\simeq U_p\sin^4\theta\langle b_\uparrow,b_\downarrow|p_\uparrow^\dagger p_\uparrow p_\downarrow^\dagger p_\downarrow|b_\uparrow,b_\downarrow\rangle, \tag{3.8}$$

where $p$ refers to the relevant oxygen $p$ orbital (i.e., either $p_x$ or $p_y$) on the oxygen site bridging the two copper sites. The matrix element in this form has a simple physical interpretation. The factor $\sin^4\theta$ is the probability that both holes occupy a $b$ orbital and the last factor is the further probability that the bridging oxygen is doubly occupied. (Actually this is not quite correct since there will be a small probability of double occupation of other sites. See below.) Now a hole in an oxygen $b$ orbital spends approximately 1/4 (actually slightly less) of its time on the four oxygen sites surrounding the copper. Hence $\langle b_\uparrow,b_\downarrow|p_\uparrow^\dagger p_\uparrow p_\downarrow^\dagger p_\downarrow|b_\uparrow,b_\downarrow\rangle\simeq 1/16$, resulting in

$$|J_p|\simeq\frac{1}{8}U_p\sin^4\theta<\frac{1}{32}U_p, \tag{3.9}$$

where the last inequality follows since the probability $\sin^2\theta$ of oxygen occupation in the single-hole cell state is always less than that of copper for the cases of interest. It is these ''reduction factors'' for double occupation of oxygen which render the cell perturbation scheme convergent, even when $U_p$ is quite large. Starting from $H_p$ in $d$-$b$ representation, Eq. (2.8), which accounts for double occupation of oxygen sites in addition to the bridging oxygen, gives

$$J_p=-2\psi_{0011}U_p\sin^4\theta=-0.1179U_p\sin^4\theta, \tag{3.10}$$

rather than (3.9), justifying the above reasoning. (Also, coefficients $\psi_{iijj}$ for further neighbors are indeed much smaller). From Eq. (3.10) it follows immediately that, for fixed $U_p$, the magnitude of the first-order contribution is strongly dependent on $\bar{\varepsilon}$, since

$$\sin^4\theta=\frac{1+2x^2-2x\sqrt{1+x^2}}{4(1+x^2)}, \tag{3.11}$$

where $x=\bar{\varepsilon}/(4\mu_{00}t_{pd})=\bar{\varepsilon}/(3.8324\ t_{pd})$.

We now consider higher-order corrections to this spin-dependent (Heisenberg) interaction. As shown in Ref. 14, the most important correction, which is accounted for very accurately in second order, is due to double cell occupation (as intermediate state) of the ER triplet. It arises from the processes $|\sigma,\bar{\sigma}\rangle\rightarrow|0,T_0\rangle\rightarrow|\bar{\sigma},\sigma\rangle$ and $|\sigma,\bar{\sigma}\rangle\rightarrow|0,T_0\rangle\rightarrow|\sigma,\bar{\sigma}\rangle$, which contribute to $j_{ij}$ and $\bar{v}_{ij}^{gg}$, respectively, and $|\sigma,\sigma\rangle\rightarrow|0,T_{2\sigma}\rangle\rightarrow|\sigma,\sigma\rangle$, which contributes to $v_{ij}^{gg}$. [There is therefore also a separate spin-independent interaction generated; compare Eq. (3.2)]. As with the first-order contribution, this gives rise to a ferromagnetic Heisenberg interaction which is independent of $U_d$, but, unlike the first-order contribution, it is also nearly independent of $U_p$ (since double occupation of oxygen is not allowed in the triplet state, so that only the hopping parameter involved, $t^{Tg0g}$, depends weakly on $U_p$, but the energy denominator $E_T+E_0-2E_g$ does not). There are also (antiferromagnetic) contributions from the other two-hole states (i.e., the singlets $|S'\rangle$ and $|S''\rangle$), which do give rise to a $U_d$ and $U_p$ dependence, though mainly $U_d$. In Fig. 8 we plot these second-order corrections (for $V_{pd}=U_p=0$), showing explicitly its variation with $\bar{\varepsilon}$, and demonstrating the dependence on $U_d$ and the significant effect of oxygen bandwidth. The latter we expect because $t_{pp}$ must enhance the hopping parameters involved.

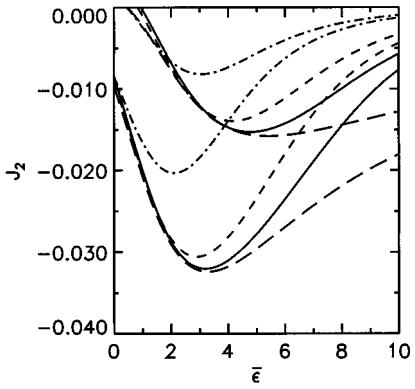


FIG. 8. Second-order contribution $J_2$ to single-band exchange $J_{\rm SB}$ vs $\bar{\varepsilon}$ for $U_d=2$ (dot-dashed line), $U_d=5$ (dashed line), $U_d=7$ (solid line), $U_d=\infty$ (long-dashed line), and $V_{pd}=U_p=0$, showing also the effect of finite oxygen bandwidth: $t_{pp}=0$ (upper curves), $t_{pp}=0.5$ (lower curves).

In Fig. 9 we plot the total exchange for the effective single-band model, i.e., including both first-order and second-order contributions, for various $U_p$ and $V_{pd}$ at

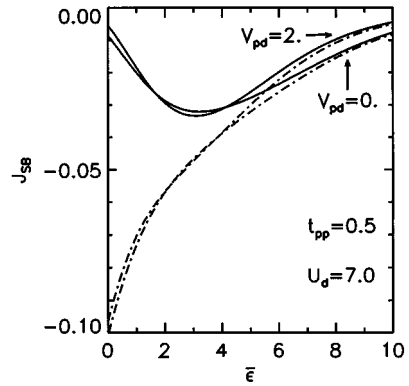


FIG. 9. Exchange in single-band model, $J_{\rm SB}$, vs $\bar{\varepsilon}$, for $U_p=0$ (solid line) and $U_p=3$ (dot-dashed line) for $V_{pd}=0$ and $V_{pd}=2$ as indicated, for $U_d=7$.

$U_d=7$ (the behavior for other $U_d$ being similar). This shows how $U_p$ can induce a large $\bar{\varepsilon}$ dependence (through the first-order contribution) for $\bar{\varepsilon}\lesssim 4$, whereas the $\bar{\varepsilon}$ dependence at larger $\bar{\varepsilon}$, coming almost entirely from the second-order contributions, is much weaker. Note further that $V_{pd}$ suppresses the ferromagnetic exchange at large $\bar{\varepsilon}$ by enhancing the hopping parameters connecting to the singlets, but that its effect is negligible for small $\bar{\varepsilon}$, in particular for parameters corresponding to the cuprates. Figure 9 further shows that in general the total exchange parameter in the effective single-band model is given to a very good approximation by

$$J_{\mathrm{SB}}=J_1(\bar{\varepsilon},U_p)+J_2(\bar{\varepsilon},t_{pp},U_d,V_{pd}), \tag{3.12}$$

where $J_1$ is the first order contribution, linear in $U_p$ as discussed above, and $J_2$ is the second-order contribution and almost independent of $U_p$. We further see that for the parameters corresponding to the cuprates, these first- and second-order contributions are of a similar order. As with the next-nearest-neighbor hopping above this merely reflects that they arise from physically distinct processes, and does not indicate poor convergence of the perturbation expansion.

### E. Effective Coulomb interactions

In addition to $U_{\mathrm{eff}}$, the effective ''on-cell'' Coulomb repulsion discussed above, there are further *intercell* effective Coulomb interactions which are potentially important. These effective interactions depend, of course, on all the parameters in the underlying $d$-$p$ model but, as we shall see, they depend most crucially on the charge-transfer gap $\varepsilon=\varepsilon_p-\varepsilon_d$ and the nearest-neighbor Coulomb repulsion $V_{pd}$. This is not surprising since extensive studies of the $d$-$p$ model indicate that its behavior can be fundamentally different when $V_{pd}/\varepsilon$ is sufficiently large, possibly leading to phase separation,[21,23,50] superconductivity,[5,51–60] or non-Fermi-liquid behavior.[61–65] We shall not consider the possibility of such behavior in this paper but will simply point out the equivalence to an effective single-band model and show the dependence of the effective Coulomb parameters on those of the underlying $d$-$p$ model.

In Eq. (3.1) the effective Coulomb ($v$) parameters represent the direct interaction (repulsion) between electrons, holes, and spins on neighboring cells. In the region of interest, for which the number of sites with electrons and/or holes is small compared with sites with spins, the physically important quantities are the *differences* in energies when the mobile carriers (electrons and holes) are on neighboring cells compared with when they are far apart. Consider, for example, the case of two holes in a background of spins. When the holes are far apart they each interact with four neighboring spins through the Coulomb term $v_{01}^{Sg}$ in Eq. (3.1). When they are on neighboring cells, they each interact with three neighboring spins and with each other through $v_{01}^{SS}$ and there is also an extra spin-spin bond in the system. Hence, the interaction energy between two holes on neighboring cells relative to when they are far apart is

$$V_{01}^{hh}=v_{01}^{SS}+v_{01}^{gg}-2v_{01}^{Sg}. \tag{3.13}$$

This relative interaction energy, and the corresponding expressions for two electrons, and an electron and hole, may be made explicit in the effective Hamiltonian by eliminating the electron-spin and hole-spin interactions through the identity

$$X_i^{gg}+X_i^{00}+X_i^{SS}=\mathbb{1}_i. \tag{3.14}$$

Using this in Eq. (3.1) leads directly to the following expression for $H_{\mathrm{eff}}$ in first order [apart from an unimportant overall constant which is dropped; cf. Eq. (3.1)]:

$$H_{\mathrm{eff}}=(\bar{E}_g-E_0)\sum_i X_i^{gg}+[2(\bar{E}_g-E_0)+\bar{U}_{\mathrm{eff}}]\sum_i X_i^{SS}$$
$$+T_{\mathrm{eff}}+H_{\mathrm{spin}}^{(p)}+\sum_{\langle ij\rangle}[V_{ij}^{ee}X_i^{00}X_j^{00}+V_{ij}^{hh}X_i^{SS}X_j^{SS}+V_{ij}^{eh}(X_i^{00}X_j^{SS}+X_i^{SS}X_j^{00})], \tag{3.15}$$

where $T_{\mathrm{eff}}$ are the hopping terms and have the same form as in (3.1), $H_{\mathrm{spin}}^{(p)}$ are the spin-dependent terms given by Eq. (3.7), and

$$\bar{E}_g=E_g-\sum_{j(\neq 0)}(v_{0j}^{0g}-v_{0j}^{gg}), \tag{3.16}$$

$$\bar{U}_{\mathrm{eff}}=U_{\mathrm{eff}}+\sum_{j(\neq 0)}(v_{0j}^{Sg}+v_{0j}^{0g}-2v_{0j}^{gg}), \tag{3.17}$$

$$V_{ij}^{ee}=v_{ij}^{00}+v_{ij}^{gg}-2v_{ij}^{0g}, \tag{3.18}$$

$$V_{ij}^{hh}=v_{ij}^{SS}+v_{ij}^{gg}-2v_{ij}^{Sg}, \tag{3.19}$$

$$V_{ij}^{eh}=v_{ij}^{0S}+v_{ij}^{gg}-v_{ij}^{0g}-v_{ij}^{Sg}, \tag{3.20}$$

where the $v$ matrix elements were defined in the previous section.

In the usual single-band Hubbard model supplemented by a nearest-neighbor Coulomb interaction $\Sigma_{\langle ij\rangle}Vn_in_j$ one has $v^{00}=v^{0g}=v^{0S}=0$, $v^{gg}=V$, $v^{Sg}=2V$, and $v^{SS}=4V$, giving

$$V^{ee}=V^{hh}=-V^{eh}=V; \tag{3.21}$$

i.e., electron-electron repulsion, hole-hole repulsion, and electron-hole attraction are all equal in magnitude. This is not usually true for the interactions between the effective holes $|S\rangle$ and electrons $|0\rangle$ we are considering here and it is this *asymmetry in the V's* (and the *t*'s) which is the main difference between the usual single-band model and the effective single-band models derived from multi-band models. We further note that this asymmetry also leads to a renormal-

ization of the on-cell effective Coulomb repulsion (and hence the Mott-Hubbard gap), as seen directly from Eq. (3.17), whereas this is unaffected by $V$ in the ordinary Hubbard model as pointed out recently by Meinders *et al.*,[66,67] clarifying some earlier confusion on this issue.[68,69] For the ''standard'' cuprate parameters the renormalization is rather small: we find $U_{\rm eff}\approx 2.6$ (as compared to $U_{\rm eff}\approx 2.5$) corresponding to $\approx 3.4$ eV.

We now derive explicit expressions for the dependence of these effective Coulomb interactions between electrons and holes on the underlying Coulomb interactions in the $d$-$p$ model, starting with $V_{pd}$. This gives a contribution in first order, which is obtained from the $d$-$b$ representation of $H_{pd}$, i.e., the first term in Eq. (2.7):

$$H_{pd}^{\rm Coul}=V_{pd}\sum_{i,j}{}' \phi_{ijj} n_i^{(d)} n_j^{(b)} . \tag{3.22}$$

The on-cell term ($\phi_{000}=0.9180$) is already included in the diagonalization of the two-hole cell states and need not be considered further. The only relevant intercell interaction term is that for nearest neighbors with coefficient $\phi_{011}=0.2430$, since this is much larger than any other coefficient ($\phi_{022}=0.0094$, etc.). With this nearest-neighbor approximation (and dropping therefore cell indices from now on) we can easily calculate the corresponding $v$ matrix elements appearing in (3.1), having first obtained the cell eigenstates $|0\rangle, |g_\sigma\rangle$, and $|S\rangle$ by explicit diagonalization, i.e.,

$$v_{pd}^{\nu\mu}=V_{pd}\phi_{011}(n_\nu^{(d)} n_\mu^{(b)}+n_\mu^{(d)} n_\nu^{(b)}), \tag{3.23}$$

where $\nu,\mu=0, S$, or $g$, with $n_\nu^{(d)}\equiv\langle\nu|n^{(d)}|\nu\rangle$, etc. Hence the Coulomb matrix elements are determined by the $d$ and $b$ densities of the cell states involved. Note that for two- (or more-) hole states, these densities depend themselves also on $V_{pd}$, and the dependence of the $v$'s on $V_{pd}$ is thus nonlinear.

Inserting the expression (3.23) into Eqs. (3.18), (3.19), and (3.20), we obtain

$$\begin{aligned} V_{pd}^{ee}&=2V_{pd}\phi_{011}(n_0^{(d)}-n_g^{(d)})(n_0^{(b)}-n_g^{(b)}) \\ &=2V_{pd}\phi_{011}n_g^{(d)}n_g^{(b)}, \end{aligned} \tag{3.24}$$

$$V_{pd}^{hh}=2V_{pd}\phi_{011}(n_S^{(d)}-n_g^{(d)})(n_S^{(b)}-n_g^{(b)}), \tag{3.25}$$

and

$$\begin{aligned} V_{pd}^{eh}&=V_{pd}\phi_{011}[(n_S^{(d)}-n_g^{(d)})(n_0^{(b)}-n_g^{(b)})+(d\leftrightarrow b)] \\ &=-V_{pd}\phi_{011}[(n_S^{(d)}-n_g^{(d)})n_g^{(b)}+(n_S^{(b)}-n_g^{(b)})n_g^{(d)}], \end{aligned} \tag{3.26}$$

showing that, as one would expect, the effective Coulomb interaction between doped particles is precisely the interaction between the *added* charges. Since the copper vs oxygen character of an added hole (i.e., $n_S^{(d)}-n_g^{(d)}$ vs $n_S^{(b)}-n_g^{(b)}$) will usually be different from that of an added electron (i.e., a removed hole, $n_g^{(d)}$ vs $n_g^{(b)}$), in general $V_{pd}^{hh}$, $V_{pd}^{ee}$, and $-V_{pd}^{eh}$ will not be equal. In particular, because $\phi_{011}>0$, it follows from these equations that the electron-electron interaction is always repulsive and the electron-hole interaction is generally attractive, as with the ordinary Hubbard model containing a nearest-neighbor Coulomb repulsion $V$ [see Eq. (3.21)]. However, the hole-hole interaction can be either *attractive or repulsive*, depending on the values of the densities, which in turn are determined by the hybridization of the states $|S\rangle$ and $|g_\sigma\rangle$. [This should again be contrasted with the ordinary Hubbard model where the hole-hole interaction is always repulsive, Eq. (3.21).] We illustrate this in Figs. 10(a) ($V_{pd}=1$) and 10(c) ($V_{pd}=2$), which are contour plots of $V^{hh}$ in the ZSA ($U_d,\bar{\varepsilon}$) diagram. [These plots also contain second-order corrections (see below).] They show the crossover from repulsive to attractive interaction as we move from the bottom right of the diagrams (i.e., Mott-Hubbard regime) to the top left (i.e., charge-transfer regime), with the attractive region increasing with $V_{pd}$.

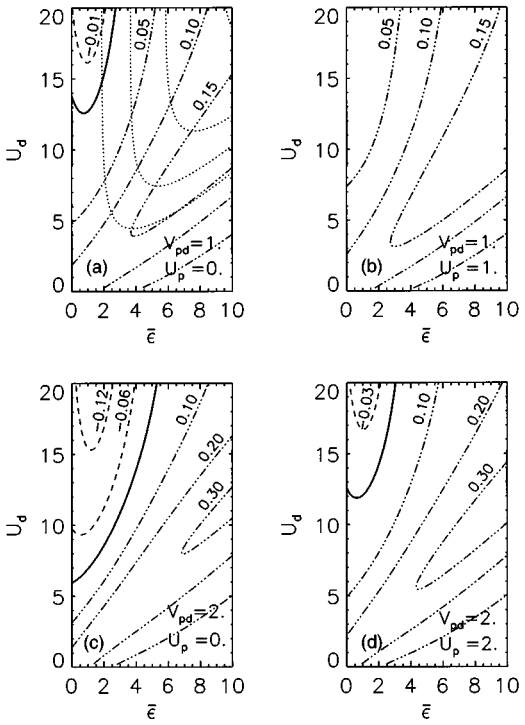


FIG. 10. Contour plots of effective hole-hole interaction $V^{hh}$ vs $U_d$ and $\bar{\varepsilon}$. Solid line is where $V^{hh}=0$, and $V^{hh}$ is attractive above this (dashed lines) and repulsive below (dot-dashed lines) as indicated. The dotted lines in (a) are contours for $U_p=V_{pd}=0$, increasing from 0.025 (bottom left) to 0.100 (top right). (a) $V_{pd}=1, U_p=0$, (b) $V_{pd}=1, U_p=1$, (c) $V_{pd}=2, U_p=0$, (d) $V_{pd}=2, U_p=2$.

This behavior can be understood as follows. As is well known, in the charge-transfer regime the holes present in the undoped system are predominantly $d$ like, but in going from the one-hole state to the ZR singlet the increase in $p$ density is larger than the increase in $d$ density because of the copper Coulomb repulsion (''the second hole is more oxygen like than the first''); i.e., the ZR singlet is more hybridized than the one-hole state. It is actually possible that $n_S^{(d)}<n_g^{(d)}$; i.e. when a hole is added, the $p$ density increases by more than one hole while the $d$ density *decreases.* This can occur because the intracell interaction generated by $V_{pd}$ suppresses the amplitude of the $pd$ singlet in the ZR singlet, i.e., forces the charge to go on oxygen, when $\bar{\varepsilon}/t_{pd}$ is small enough (and $U_d$ sufficiently larger than $\bar{\varepsilon}$). Under these conditions, i.e., in the extreme CT regime close to the $dp$-metal region in the

ZSA phase diagram, it is favorable for two ZR singlets to share this $d \rightarrow p$ CT polarization. Since they are both very oxygen like, the $pd$ repulsion between them is then very weak, much weaker than the repulsion experienced by a ZR singlet from a background $g$ state.

In this context it should be pointed out that the CT regime, usually understood[33] as $U_d > \varepsilon$, can be subdivided in two rather distinct subregions, separated by the line $U_d = 2\bar{\varepsilon} + U_b$ in the ZSA diagram. At this line $n_S^{(d)} = n_S^{(b)} = 1$, as follows immediately from the Hamiltonian matrix determining $|S\rangle$ [see Appendix B of II, Eq. (B2)], so that $n_S^{(d)} - n_g^{(d)} = 1 - n_g^{(d)} = n_g^{(b)}$ and $n_S^{(b)} - n_g^{(b)} = n_g^{(d)}$, and thus the $V_{pd}$ generated effective Coulomb interactions show electron-hole symmetry, $V_{pd}^{hh} = V_{pd}^{ee}$ (although $V_{pd}^{eh} = -V_{pd}^{hh} - V_{pd}\phi_{011}\cos^2 2\theta \neq -V_{pd}^{hh}$). Below the dividing line the ZR singlets are still predominantly $d$ like, although less so than the one-hole states, while above it the oxygen $p$-hole content of the ZR singlets is larger than the copper $d$-hole content. Simple algebra then shows that $V_{pd}^{hh} > V_{pd}^{ee}$ below that line, while above it $V_{pd}^{hh} < V_{pd}^{ee}$. It is only in the latter region that $V_{pd}^{hh}$ can possibly be attractive and it is noteworthy that the cuprates are actually in that region. However, it should be pointed out that, even for $U_p = 0$ as shown in Figs. 10(a) and 10(c), the region of *attraction only occurs for relatively large values of* $U_d$ (and even larger $U_d$ when $U_p \neq 0$; see below). Also, to obtain an attraction of a given strength requires much larger $V_{pd}$ at finite $U_d$ than at $U_d = \infty$. Theoretical treatments which set $U_d = \infty$ (applications of the slave boson method, for example, both to the $d$-$p$ model proper[21,23] and to the multi-band $t$-$J$ models derived from it[70,71]), therefore tend to overestimate the tendency towards phase separation or superconductivity induced by effective hole-hole attraction. In the opposite (Mott-Hubbard) case where $U_d < \bar{\varepsilon}$ the situation is more straightforward since the charge will shift to the $d$ orbital and $V^{hh}$ is always repulsive.

We now consider the first-order contribution made by $U_p$, which may be analyzed by the same reasoning. The appropriate effective Coulomb interaction is given in the first sum of Eq. (2.8), i.e.,

$$H_p^{\mathrm{Coul}} = U_p \sum_{ij}{}' \psi_{iijj} n_{i\uparrow}^{(b)} n_{j\downarrow}^{(b)} . \tag{3.27}$$

Again, the large on-cell term ($\psi_{0000} = 0.2109$) is already absorbed in the single-cell Hamiltonian, which is diagonalized explicitly. As explained in the section on spin-dependent terms, the nearest-neighbor two-cell interactions (with $\psi_{0011} = 0.0590$) are by far the largest since these arise from two holes on the bridging oxygen site ($\psi_{0022} = 0.0044$, etc.). Retaining only these, the effective Coulomb matrix may be calculated as with the $V_{pd}$ interactions and we get

$$v_p^{\mu\nu} = U_p \psi_{0011} (n_\mu^{(b\uparrow)} n_\nu^{(b\downarrow)} + n_\mu^{(b\downarrow)} n_\nu^{(b\uparrow)}) . \tag{3.28}$$

For $\mu = g_\sigma$, $\nu = g_{\bar{\sigma}}$, this Coulombic term, when combined with the spin-dependent terms in $H_p$ [see Eq. (2.8)], gives rise to the exchange contribution discussed earlier, and thus makes no contribution to the spin-independent interactions we are now considering. The terms originating from other combinations of $\mu$ and $\nu$, when inserted into Eqs. (3.18), (3.19), (3.20), yield

$$V_p^{ee} = 0, \tag{3.29}$$

$$V_p^{hh} = U_p \psi_{0011} (\tfrac{1}{2} n_S^{(b)} - n_g^{(b)}) n_S^{(b)} , \tag{3.30}$$

$$V_p^{eh} = -\tfrac{1}{2} U_p \psi_{0011} n_S^{(b)} n_g^{(b)} . \tag{3.31}$$

The nonsymmetric form of these expressions is the result of our including part of the spin-independent interaction, viz., $\frac{1}{2} U_p \psi_{0011} (n_g^{(b)})^2$, with the exchange [compare Eqs. (3.7) and (3.10)]. The full spin-independent interaction has $V_p^{ee} \propto (n_g^{(b)})^2$, $V_p^{hh} \propto (n_S^{(b)} - n_g^{(b)})^2$, and $V_p^{eh} \propto (n_S^{(b)} - n_g^{(b)}) n_g^{(b)}$, which is again interpretable as the interaction between the *added* charges. Since $\psi_{0011} > 0$, we find that the effective Coulomb interaction between neighboring cells due to $U_p$ is always attractive between electrons and holes and repulsive between ZR singlets throughout the charge-transfer regime in the ZSA diagram. As argued above, this is because the presence of $U_d$ guarantees that $n_S^{(b)} > 2 n_g^{(b)}$. Physically the repulsion comes about because nearest-neighbor ZR singlets, in optimizing hybridization and avoiding the copper Coulomb repulsion, necessarily pile up charge on the oxygen atom bridging the two copper sites. Actually, $U_p$ suppresses attraction between ZR singlets much more effectively than would be expected from Eq. (3.30) alone. The oxygen Coulomb repulsion not only generates the intercell interaction (3.30) but also modifies the wave function of the two-hole state $|S\rangle$ through the *intracell* term. This rapidly reduces the oxygen hole content of the ZR singlet, thus counteracting the effect of $V_{pd}$. The effect of $U_p$ is demonstrated in Figs. 10(b) and 10(d), where the region of attractive $V^{hh}$ is seen to be shifted to considerably higher values of $U_d$ compared to $U_p = 0$. However, this suppression of an effective hole-hole attraction is overestimated somewhat in the present treatment, because the ZR singlets are not allowed to relax, i.e., to modify their wave function, when brought next to one another.

Of course there are also second-order contributions (included in Fig. 10), arising in perturbation theory. These may be interpreted, in view of Eqs. (3.18), (3.19), and (3.20), as the difference in self-energy between an added particle (say, a hole, i.e., a ZR singlet) placed next to another particle or surrounded only by spins (i.e., one-hole cells), and arising from the different virtual transitions that are available.[14,26] These interactions, which are already generated in the pure Emery model (i.e., with $V_{pd} = U_p = 0$) are always repulsive [see Fig. 10(a), dotted lines], essentially because the number of virtual states available is larger when the particle is next to a one-hole cell. For example, for a ZR singlet, $Sg \rightarrow \underline{g}0, \underline{e}0; \underline{g}T, \underline{g}S', gS'', \underline{e}S, \underline{e}T, \underline{e}S', \underline{e}S''$, as compared with $SS \rightarrow \underline{g}g, \underline{g}e, \underline{e}g, \underline{e}e$ (where $\underline{g}$ and $\underline{e}$ denote the three-hole ground and excited state). Moreover $Sg \rightarrow gT$ is a relatively low-energy excitation, thus making a significant contribution to the effective interaction between neighboring ZR singlets. Since these second-order contributions can be appreciable, the choice made for the ''background'' is important here. If a zero-hole background is assumed, i.e., if the ''indirect'' terms in Eqs. (3.4) and (3.5) are omitted, the second-order repulsive contribution is considerably weaker because the effective hopping parameters are reduced, leading to a much larger attractive regime in the ZSA diagram.

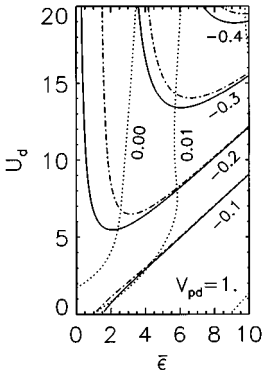


FIG. 11. Contour plot of effective electron-hole interaction $V^{eh}$ vs $U_d$ and $\bar{\varepsilon}$ for $V_{pd}=1$. Solid lines are for $U_p=0$ and dot-dashed lines for $U_p=3$. ($U_p=V_{pd}=0$ is shown as a dotted line.)

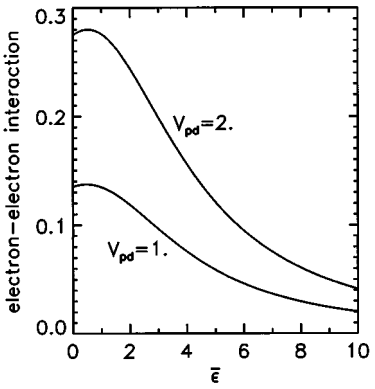


FIG. 12. Effective electron-electron repulsion $V^{ee}$ vs $\bar{\varepsilon}$.

As regards the cuprates, Fig. 10 shows that for $U_p=0$, in spite of the repulsive second-order terms, a net attractive interaction between ZR singlets can still be induced by a $V_{pd}$ of order 1–2 eV (as estimated for the cuprates[37–41,72]) in the extreme CT regime close to the $dp$-metal region in the ZSA diagram. One must further bear in mind that $V_{pd}$ increases $U_{\rm eff}$ (see Fig. 4) and thus the charge-transfer gap, so that in order to describe a system with a particular gap value, one has to decrease $\bar{\varepsilon}$ when increasing $V_{pd}$, thus coming closer to (or within) the attractive regime in Fig. 10. However, attraction occurs only at fairly large values of $U_d$, and although *the first-order interaction generated by $V_{pd}$ is clearly attractive in the region where the cuprates are estimated to be located* ($U_d/t_{pd}\approx 7$, $\bar{\varepsilon}/t_{pd}\approx 2$ when $V_{pd}=0$), it is obvious from Figs. 10(a) and 10(c) that a net attraction is already doubtful when the second-order corrections are included. Moreover, Figs. 10(b) and 10(d) show that the attraction is rapidly suppressed by the oxygen Coulomb interaction, and for realistic $U_p$ (3–6 eV, taking screening into account[37–41]) the interaction is likely to be *repulsive* even without the second-order contributions, and certainly so when they are included. For example, for the "standard" cuprate parameter set we find $V^{hh}=+0.17$ eV. In this respect it is noteworthy that investigations into the effect of $V_{pd}$ have sometimes been done for $U_p=0$,[21,22,58] (and occasionally also with $U_d=\infty$ where the condition for attractive interaction is considerably less stringent than for realistic $U_d$). Phase separation or superconducting correlations found in such studies, if induced by effective hole-hole attraction, may then not survive for a more realistic choice of parameters, or only in a more restricted range of doping. For example, stabilization of the system against phase separation by $U_p$ has been found explicitly in the high doping regime.[23,70,71]

However, we should also point out that a negative $V^{hh}$ does *not* necessarily imply that the holes will be attracted to each other; nor does a positive $V^{hh}$ imply that they will not. For one thing these are only static interactions which, of course, have to compete with the kinetic energy (hopping) terms in determining the phase behavior of the system. In addition to this, the ferromagnetic Heisenberg interaction, arising from the $U_p$ interaction in first order and the Emery triplet in second order, will lead to an effective repulsion between holes. This is [compare Eq. (3.2)] because the Heisenberg interaction contributes for any two adjacent spins an energy lying between zero and $-J_{\rm SB}$ ($>0$) and this energy only vanishes when the spins are ferromagnetically aligned (a situation which does not arise for the cases of interest). Hence, the system may lower its (static) energy by minimizing the number of pairs of sites which are occupied with spins. For a given number of holes, this occurs when the holes do not occupy adjacent sites. Thus this ferromagnetic interaction between spins is equivalent to a repulsive interaction between holes. Indeed, this is just the other (spin-dependent) part of the effective cell-cell interaction due to $U_p$ further suppressing any attraction (as does $V_p^{hh}$). (See also Sec. IV B for a further discussion of effective hole-hole interactions.)

In Fig. 11 we show the effective electron-hole interaction $V^{eh}$, including the second-order contributions. The calculations show that it is strongly dominated by the first-order $V_{pd}$ contribution, the contributions from second order and from $U_p$ being relatively small (as can be seen in the figure). It is also clear that strong excitonic effects should be expected as soon as $V_{pd}$ were large enough to generate any sizable hole-hole attraction in the extreme charge-transfer regime (compare Fig. 10). Finally, Fig. 12 shows the electron-electron interaction $V^{ee}$ which, as already mentioned, is always repulsive. The repulsion is independent of $U_d$, and almost independent of $U_p$ which affects only the effective hopping parameters entering the second-order contributions. Comparison with Fig. 10 reveals the considerable difference from the hole-hole interaction, except in the extreme Mott-Hubbard regime ($\bar{\varepsilon}\gg U_d$) where of course all Coulomb interactions related to oxygen occupation tend to zero. In particular the magnitude of $V^{ee}$ is seen to be quite large in the charge-transfer regime precisely where the hole-hole interaction is weak.

We thus see that there is a strong asymmetry between doped holes and doped electrons as far as the residual interactions are concerned, in particular in the extreme CT regime. This is to be contrasted with the behavior of the hopping (Sec. III C) and the single-particle spectral properties,[73,74,31] where precisely in that regime electron-hole symmetry is almost completely restored by the hybridization. We emphasize that the presence of these *asymmetric effective Coulomb interactions* represents a significant qualitative difference between an effective single-band model derived from the three-band $d$-$p$ charge-transfer model and the ordinary Hubbard model.

### F. Insulator-metal transition

In Sec. III B we showed that the reduction of the *d-p* model to an effective single-band model by perturbation theory is valid over a wide range of parameters and that the effective single-band parameters are given to reasonable accuracy in second order. For the special case of one hole per cell (on average) it is clear that this parameter range for which the mapping is valid includes metallic as well as insulating regimes. In fact, for the regime which is expected to be metallic (small $U_d$ and/or small $\bar{\varepsilon}$) the expansion parameters are actually smaller and truncation at second order is more accurate. The case of the charge-transfer metal is particularly interesting. If we go back to the *d-p* model, then we expect to get metallic behavior when $\varepsilon_p-\varepsilon_d$ becomes comparable with $t_{pd}$ or smaller and charge will ''transfer'' from Cu to O where it becomes mobile. How can this simple picture be reconciled with an effective single-band model? It might be expected that the two descriptions are incompatible since, if the mobile holes on oxygen were to execute their normal band motion, then we would expect cell states with three or more holes to become important, whereas the effective single-band model only allows unoccupied, singly occupied, or doubly occupied (in Zhang-Rice singlets) cell states. The reason that the effective single-band description remains valid down to $\varepsilon_p-\varepsilon_d\approx 0$ is due to the strong effect of Cu-O hybridization ($t_{pd}$) which pushes down the energy of single-hole and two-hole (ZR) cell states, leaving cell states with three or more holes sufficiently high in energy to be accounted for as small perturbative corrections. The physics is that the system can already gain energy significantly by hybridizing only *locally*, rather than promoting holes to band states, thus avoiding the higher price of Coulomb energy that would result from a large amplitude for double Cu (and O) occupancy. There are, of course, regimes where this would break down and a more appropriate description would be an oxygen band perturbed by the Cu spins. An example would be $t_{pd}\ll t_{pp}$, which is appropriate for heavy fermion and mixed valence compounds (with $p\mapsto d$ and $d\mapsto f$) for which an effective single-band model would certainly *not* be valid. The description would also eventually break down for $\varepsilon_p-\varepsilon_d$ sufficiently negative since the hybridization effects of $t_{pd}$ would become smaller and again a weakly perturbed oxygen band of mobile holes would become more appropriate. However, for the range of parameters considered in this paper, with $t_{pp}/t_{pd}=0.5$ and $\varepsilon_p-\varepsilon_d\geqslant 0$, the equivalence of the *d-p* model to an effective single-band model remains valid and *includes both insulating and metallic regimes.* This thus spans the insulator-metal (IM) transition.

The precise region where the IM transition occurs is not known even for the ordinary Hubbard model, though it is expected to occur for a critical ratio of $8t/U$ of around unity.[75] This may be justified by the simple (but approximate) argument that it requires an energy $U$ to create an electron-hole pair in the atomic limit. The electron and hole can each further lower their energies by half the bandwidth [i.e., $4t$ in a two-dimensional (2D) system] giving a net creation energy of $U-8t$, which vanishes at the IM transition. Since correlations between the mobile particles and the spin background are known to reduce the effective bandwidth, one underestimates the gap in this way and the critical value of $8t/U$ will actually be somewhat larger than 1. If we apply a similar argument to the effective single-band model derived above [see Eq. (3.15)], then the appropriate ratio is $4(t^{ee}+t^{hh})/U_{\rm eff}\approx 8t^{eh}/U_{\rm eff}$ and we expect an IM transition when this ratio is of order unity. In Fig. 13 we present contour (ZSA) plots of this ratio versus $U_d$ and $\bar{\varepsilon}$ for various $U_p$ and $V_{pd}$ with $t_{pp}=0.5$. This shows clearly the crossover from Mott-Hubbard behavior (large $\bar{\varepsilon}$) to CT behavior (large $U_d$) with the parameters corresponding to the cuprates being in the CT regime, but not significantly so. Furthermore, the cuprates correspond to $8t^{eh}/U_{\rm eff}\approx 1$, i.e., quite close to the expected IM transition regime. Note that the Coulomb interactions $U_p$ and $V_{pd}$ shift the contours to the left in the CT region because they significantly increase $U_{\rm eff}$ (see Fig. 4), but have little effect in the Mott-Hubbard region. This agrees with the general expectation that these Coulomb interactions inhibit kinetic energy but are only effective when the probability of oxygen occupation is high. A more detailed study of the effect of $V_{pd}$ and $U_p$ within the Hubbard I approximation has recently been made by Simón *et al.*[29,30]

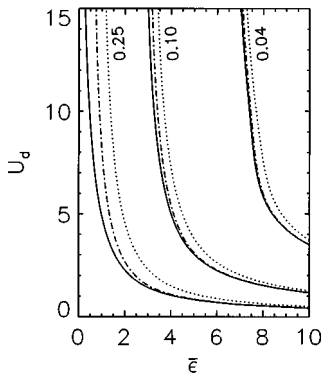


FIG. 13. Contour plots of $t^{eh}/U_{\rm eff}$ vs $U_d$ and $\bar{\varepsilon}$ for $U_p=V_{pd}=0$ (dotted lines), $V_{pd}=1$, $U_p=0$ (dot-dashed lines), and $V_{pd}=1$, $U_p=3$ (solid lines).

## IV. FURTHER REDUCTION TO A CHARGE-SPIN MODEL

### A. *t-J-V* model

In much the same way as the ordinary Hubbard model may be reduced to the *t-J* model[76] for $U/t\gg 1$, the effective single-band model derived from the *d-p* model in the previous section may be reduced to a charge-spin model provided $U_{\rm eff}$ is sufficiently large. Applying second-order degenerate perturbation theory to (3.15) leads directly to what we will call the *t-J-V* model,

$$H_{tJV}=P\left\{\sum_{\langle ij\rangle\sigma}-t_{ij}[c^{\dagger}_{i\sigma}c_{j\sigma}+\text{H.c.}]+\sum_{\langle ij\rangle}[J(\mathbf{S}_i\cdot\mathbf{S}_j-\tfrac{1}{4}n_in_j)+Vn_in_j]\right\}P, \qquad (4.1)$$

where the summations $\langle ij\rangle$ are over pairs of sites (cells), which we will restrict to nearest- and next-nearest neighbors for the hopping terms and nearest-neighbor only for the ''static'' terms. This form is *exactly* that which would result from a single-band Hubbard model with a nearest-neighbor Coulomb interaction $V$, except that we have omitted, for

clarity, the three-site terms, which occur in all cases. (These will be discussed briefly below.) Actually, such a $t$-$J$-$V$ model has recently been investigated,[77,78] considered as a natural generalization of the $t$-$J$ model.

The precise meaning of the symbols in Eq. (4.1) in the context of the generalized single-band model [Eq. (3.15)] and the quantitative differences between (4.1) and the $t$-$J$ model resulting from the ordinary single-band Hubbard model require further explanation. First, the $c$ operators in (4.1) may be regarded as ordinary Fermi operators provided $P$ forbids double occupancy, the usual convention for the $t$-$J$ model. For hole-doped materials, zero-hole states must be precluded, and since these are equivalent to two-electron states, we must choose the electron picture to adopt the usual convention. Thus $c_\sigma \equiv e_\sigma (= h_{\bar{\sigma}}^\dagger)$ and $P \equiv P^{(e)}$ precludes two-electron states. [Formally, $P^{(e)} \equiv \Pi_i (1 - n_{i\uparrow} n_{i\downarrow})$.] Conversely, for electron-doped materials, two-hole states must be precluded and we thus retain the hole picture with $c \equiv h$ and $P \equiv P^{(h)}$. The correctness of (4.1) is then proved formally by first obtaining $H_{tJV}$ in its $X$ operator form [directly from (3.15) using second-order perturbation theory] and then invoking the identities $X_i^{S\sigma} X_j^{\sigma S} = (h_{i\sigma}^\dagger h_{i\sigma}) h_{i\bar{\sigma}}^\dagger h_{j\bar{\sigma}} (h_{j\sigma}^\dagger h_{j\sigma}) \equiv P^{(e)} e_{i\sigma} e_{j\sigma}^\dagger P^{(e)}$ (hole doped), $X_i^{\sigma 0} X_j^{0\sigma} = (1 - h_{i\bar{\sigma}}^\dagger h_{i\bar{\sigma}}) h_{i\sigma}^\dagger h_{j\sigma} (1 - h_{j\bar{\sigma}}^\dagger h_{j\bar{\sigma}}) \equiv P^{(h)} h_{i\sigma}^\dagger h_{j\sigma} P^{(h)}$ (electron doped), $X_i^{gg} X_j^{gg} \equiv P^{(\cdots)} n_i n_j P^{(\cdots)}$ (holes or electrons), $X_i^{SS} = h_{i\uparrow}^\dagger h_{i\uparrow} h_{i\downarrow}^\dagger h_{i\downarrow} = (1 - e_{i\downarrow}^\dagger e_{i\downarrow})(1 - e_{i\uparrow}^\dagger e_{i\uparrow}) \equiv P^{(e)} (1 - n_i) P^{(e)}$ (hole doped), and $X_i^{00} = (1 - h_{i\uparrow}^\dagger h_{i\uparrow})(1 - h_{i\downarrow}^\dagger h_{i\downarrow}) \equiv P^{(h)} \times (1 - n_i) P^{(h)}$ (electron doped). The relation $P^{(\cdots)} (1 - n_i) \times (1 - n_j) P^{(\cdots)} \rightarrow P^{(\cdots)} n_i n_j P^{(\cdots)}$, which is simply a shift of the single-particle energy or the chemical potential, has also been used.

Consequently, the hopping matrix elements in (4.1) are those for "holes" in the case of hole-doped materials [i.e., $t_{ij} \equiv t_{ij}^{hh} \equiv t_{ij}^{SggS}$, Eq. (3.1)] and those for "electrons" for the case of electron-doped materials (i.e., $t_{ij} \equiv -t_{ij}^{ee} \equiv -t_{ij}^{g00g}$). In the ordinary Hubbard model no distinction is made between holes and electrons since the $t$'s are the same for both, as explained in Sec. III A. Similarly, $V = V^{hh}$ for hole-doped materials and $V = V^{ee}$ for electron-doped materials [see Eqs. (3.19) and (3.18)]. Since there can be a significant asymmetry in these $t$ and $V$ parameters, we can expect at least quantitative differences between electron- and hole-doped materials and, possibly even significant qualitative differences. (We come back to this point below.) The superexchange is given by

$$J = \frac{4 (t^{eh})^2}{\bar{U}_{\text{eff}} + V^{eh}} + J_{\text{SB}}, \tag{4.2}$$

i.e., by the usual second-order expression to which we must add the ferromagnetic contribution from the effective single-band model, which arose from $U_p$ in first order and the ER triplet in second order [see Eq. (3.12)].

As already mentioned, the reduction of the single-band model (3.15) to a charge-spin model generates in addition to (4.1) also three-site hopping terms,

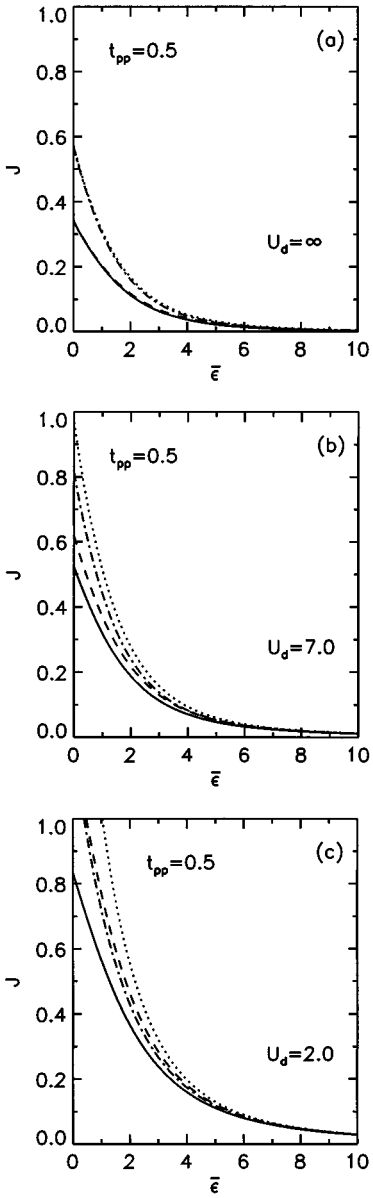


FIG. 14. Total superexchange in $t$-$J$ model for $t_{pp} = 0.5$; $V_{pd} = U_p = 0$ (dotted line), $V_{pd} = 0$, $U_p = 3$ (dashed line), $V_{pd} = 1$, $U_p = 0$ (dot-dashed line), $V_{pd} = 1$, $U_p = 3$ (solid line): (a) $U_d = \infty$, (b) $U_d = 7$, and (c) $U_d = 2$.

$$H_K^{\text{three site}} = P \Bigg\{ \sum_{ijl} \sum_\sigma [K_{lij}^{++} c_{i\sigma}^\dagger n_{l\sigma} c_{j\sigma} + K_{lij}^{--} c_{i\sigma}^\dagger n_{l\bar{\sigma}} c_{j\sigma} + K_{lij}^{+-} c_{i\bar{\sigma}}^\dagger c_{l\sigma}^\dagger c_{l\bar{\sigma}} c_{j\sigma}] \Bigg\} P. \tag{4.3}$$

Although the three-site terms are often neglected in studies of the $t$-$J$ model, they are not necessarily unimportant if one wants to consider the $t$-$J$ model as the strong-coupling ($U/t \gg 1$) limit of the ordinary Hubbard model. For example, their inclusion could make a significant difference in the formation of magnetic polarons.[79] Recently, it has also been shown that they are essential in describing the spectral weights in the optical spectra.[80,81] One expects similar arguments to apply for the present $t$-$J$-$V$ model as the strong-

coupling ($U_{\rm eff}/t^{eh} \gg 1$) limit of the $d$-$p$ model. We defer a study of the terms (4.3) to future work, and restrict ourselves here to the remark that the familiar relations between three-site hopping and superexchange[76] ($K^{++}_{lij}=0$ and $K^{--}_{lij}=-K^{+-}_{lij}=-J/4$ when $l$ is neighbor to both $i$ and $j$) are only obtained when one starts from the ordinary Hubbard model, but do not hold for the charge-spin model derived from the $d$-$p$ model.

In Fig. 14 we plot the total superexchange vs $\bar{\varepsilon}$ for various $V_{pd}$, $U_p$, and $U_d$. We see the general expected trend that increasing any of the Coulomb terms reduces $J$ by either suppressing the probability of double occupation on a cell or by reducing the effective hopping $t^{eh}$, or both. Conversely, reducing $\bar{\varepsilon}$ increases $J$ for exactly the opposite reasons. Over quite a broad range of parameters all Coulomb interactions make significant contributions. It should also be noted that, in the region of the cuprates, the ferromagnetic contribution coming from the effective single-band part of the Hamiltonian, $J_{\rm SB}$, is quite appreciable, being $\sim 20\%$ that due to the antiferromagnetic second-order term. Therefore $J$ is appreciably smaller than would be obtained from an ordinary Hubbard model with parameters $t=t^{eh}$ and $U=U_{\rm eff}$. This explains why Hybertsen *et al.*,[11] when fitting their numerical results for eigenvalues in finite clusters to a Hubbard model and comparing with cuprate data, had to increase $U$ above the value estimated from the gap in order to get a reasonable fit to the magnetic splittings. For the "standard" cuprate parameters we find $J=0.22$ eV, in reasonable agreement with earlier estimates,[9–12] though somewhat larger, and also larger than the accepted experimental value of $J \approx 0.13$ eV.[82,83] The difference could be due to the direct Cu-Cu exchange, as pointed out early on by Stechel and Jennison,[9] or might indicate that the "standard" set should be slightly modified. For example, it is well known that $J$ is very sensitive to $U_p$ (Refs. 10,27) [compare also Eq. (3.10)], and a somewhat different combination of $\varepsilon$, $U_p$, and $V_{pd}$ could bring the calculated $J$ closer to the experimental value, without appreciably changing $U_{\rm eff}$ and thus the gap.

We now consider the validity and accuracy of this second-order expansion to a charge-spin model. We see from Eq. (4.2) that an appropriate expansion parameter is $4t^{eh}/(\bar{U}_{\rm eff}+V^{eh}) \simeq 4t^{eh}/U_{\rm eff}$. This parameter was discussed in the previous section and contour plots are given for it in Fig. 13. We expect reasonably accurate second-order results when this ratio is less than unity. For the cuprates it takes a value of order 1/2 which is within the convergence radius, giving a second-order contribution to $J$ which is in error by $\approx 6\%$ (as can be estimated by comparing the exact two-cell result with the second-order result, as discussed in Ref. 14).

### B. Asymmetry: Hole doping versus electron doping

Finally let us return to the question of differences between hole-doped and electron-doped systems when both are described by Eq. (4.1), and the differences are reflected in the parameters for hopping ($t=t^{hh}$ or $t=-t^{ee}$) and nearest-neighbor effective Coulomb interactions ($V=V^{hh}$ or $V=V^{ee}$). One distinct advantage of expressing the hole-hole or electron-electron interaction in the context of an effective single-band model is that it is straightforward to make a quantitative comparison with effective attraction between added particles due to superexchange. This effective interaction has received some attention recently because of its tendency to promote phase separation[84–87] and possibly superconductivity.[88–90] This tendency is due to the fact that there is one extra magnetic bond when two carriers are on neighboring cells compared with when they are further separated, leading to an effective attraction. However, this is opposed by the kinetic energy terms which tend to favor unbound carriers and, while there is little doubt that phase separation does occur when $J/t$ is sufficiently large, whether or not this is possible for parameters appropriate to the cuprates remains an open question. One measure of the tendency to phase separation or pairing is the mean "static" energy between carriers when they are on neighboring cells compared with when they are far apart. For the pure $t$-$J$ model this is just $\Delta E_{tJ}=J(\langle \mathbf{S}_1 \cdot \mathbf{S}_2 \rangle - \frac{1}{4})$ where the angular brackets denote the expectation value with respect to some magnetic background.[91] Since $\Delta E_{tJ} \leqslant 0$, with the upper bound corresponding to a ferromagnetic background, this static interaction is generally attractive in the $t$-$J$ model with $\Delta E_{tJ}=-\frac{1}{4}J$ for a paramagnetic (PM) background and $\Delta E_{tJ}=-\frac{1}{2}J$ for an antiferromagnetic (AFM) Néel-state background. For very low doping (or for true phase separation) we might expect the background to be close to the ground state of a pure 2D Heisenberg antiferromagnet which, using the ground-state energy from quantum Monte Carlo simulations,[92] gives $\Delta E_{tJ}=-0.585J$. Thus, based on the above criterion, the pure $t$-$J$ model favors phase separation and, furthermore, there is no distinction between electron- and hole-doped systems. If we apply this same criterion to the effective charge-spin model derived from the $d$-$p$ model, Eq. (4.1), we see that the situation can be quite different due to the "spin-independent" effective Coulomb interaction term $\Sigma_{\langle ij \rangle} V n_i n_j$. Now the relevant quantity is $\Delta E_{tJV} \equiv J(\langle \mathbf{S}_1 \cdot \mathbf{S}_2 \rangle - \frac{1}{4}) + V$, where $V$ is either $V^{hh}$ or $V^{ee}$.

For electron-doped systems $V$ is always repulsive and therefore the value and in particular the sign of $\Delta E_{tJV}$ simply depend on whether this effective Coulomb repulsion is sufficiently large to cancel the attraction between electrons due to the superexchange. The resulting variation of $\Delta E_{tJV}$ with $U_d$ and $\bar{\varepsilon}$ is shown for a typical case with $V_{pd}=1$ and $U_p=0$ in Fig. 15, both for a PM and an AFM background. We see that $\Delta E_{tJV}$ is negative for either $U_d$ or $\bar{\varepsilon}$ small, where the superexchange is large (compare Fig. 14), but this attractive regime is steadily reduced with increasing $V_{pd}$ because of the continuous increase of $V$ (compare Fig. 12). In the repulsive regime the net repulsion is weak because both $J$ and $V$ are small. We further note that the type of magnetic background has a large effect, essentially because it affects only the attractive contribution, so that in a PM background a much larger $J$ and therefore a considerably smaller $\bar{\varepsilon}$ is required in order to have the same net interaction as in an AFM background.

On the other hand, for hole-doped systems $V$ can be positive or negative, so that $\Delta E_{tJV}$ can now be negative either because the attractive superexchange is larger than a repulsive effective Coulomb interaction as in the electron-doped case, or because $V$ is itself attractive and adds to $J$. As a consequence $\Delta E_{tJV}$ depends sensitively on all underlying parameters. This is illustrated in Fig. 16, where we see that in the charge-transfer regime ($U_d > \bar{\varepsilon}$) attraction persists up to

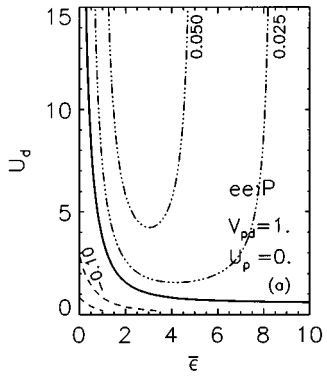


FIG. 15. Contour plots of the static electron-electron interaction $\Delta E^{ee}_{tJV}$ for (a) a paramagnetic background ($V^{ee}-\frac{1}{4}J$), (b) an antiferromagnetic background ($V^{ee}-0.585J$), for $V_{pd}=1$, $U_p=0$.

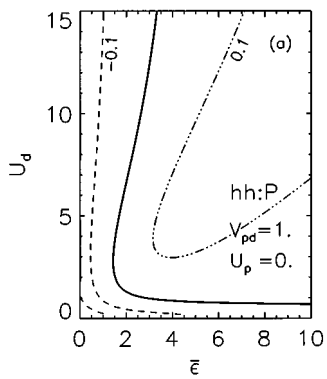


FIG. 16. Contour plots of the static hole-hole interaction $\Delta E^{hh}_{tJV}$ for (a) a paramagnetic background ($V^{hh}-\frac{1}{4}J$), (b) an antiferromagnetic background ($V^{hh}-0.585J$), for $V_{pd}=1$, $U_p=0$.

considerably larger values of $\bar{\varepsilon}$ than in the electron-doped case. This is exactly as we would expect, since it is in that regime that $V^{hh}$ becomes small or even attractive, as we have seen in Sec. III E. This difference between doped holes and doped electrons in the charge-transfer regime becomes even more pronounced at larger $V_{pd}$, where electrons become increasingly more repulsive and holes increasingly more attractive. Note further that when in the repulsive regime the repulsion between holes is much stronger than between electrons. The effect of changing the background is seen to be smaller in the hole-doped case, in particular in the charge-transfer regime, since such a change does not affect an attractive contribution from $V$ when present.

The rather different effect of the magnetic background can be seen more clearly in Figs. 17 and 18, where we show, for electrons and holes, respectively, the contours where $\Delta E_{tJV}=0$ for PM and AFM backgrounds, for two characteristic values of $V_{pd}$ and various values of $U_p$. Thus $\Delta E_{tJV}$ is negative (positive) to the left (right) of these curves. The shift of these boundaries upon going from AFM to PM is significantly smaller for holes, especially when $U_d \gg \bar{\varepsilon}$ and at the larger value for $V_{pd}$. These figures also demonstrate the large difference in the influence of $U_p$. For electrons an increase in $U_p$ has little effect, because this only reduces $J$ slightly. By contrast, in the case of holes $U_p$ makes a large repulsive contribution to $V$ as we have seen in Sec. III E, and thus the contours are shifted to significantly smaller $\bar{\varepsilon}$ where the extra repulsion is compensated by a larger value of $J$.

Note that for given $V_{pd}$ and $U_p$ there is, between the contours, a band where the static interaction would *change from attractive to repulsive* upon a change in the magnetic order of the background from AFM to PM, which is expected to occur *with increasing doping*, suggesting that a transition might occur from a phase-separated or superconductive state at low doping to a metallic state at higher doping. Figures 18(b) and 17(b) show that it is even possible that such a situation is realized for holes but not for electrons, for which the static interaction would be repulsive for any magnetic background, suggesting that such a system might support superconductivity for doped holes but not for doped electrons. Furthermore, this ''critical'' region with $\Delta E_{tJV} \approx 0$, although rather narrow for holes, can be *very close to the d-p parameter set estimated for the cuprates*.

The variation of $\Delta E_{tJV}$ with $V_{pd}$ in this boundary region is also of interest since there is a subtle cancellation of tendencies to attraction and repulsion which depends strongly on $\bar{\varepsilon}$. From Fig. 10 we see that $V_{pd}$ tends to favor attraction (or reduce repulsion) in agreement with our earlier discussions on polarization due to $d \rightarrow p$ charge transfer. However, $V_{pd}$ also reduces superexchange as shown in Fig. 14 and this reduces the effective hole-hole attraction. The result is that as $V_{pd}$ increases from zero, the quantity $\Delta E_{tJV}$ always increases at first; i.e. a more repulsive (less attractive) interaction results, due to the reduction in $J$. In the case of doped *electrons* this increase of $\Delta E_{tJV}$ simply continues, because of the simultaneous reduction of $J$ and enhancement of $V$. However, in the case of doped *holes* for $\bar{\varepsilon}$ sufficiently small ($\lesssim 2$), increasing $V_{pd}$ will reverse this trend when the attraction due to $V^{hh}$ (the charge-polarization effect) more than compensates the decrease in $J$. Again, for the expected parameters of the cuprates, $\Delta E_{tJV}$ passes through a maximum

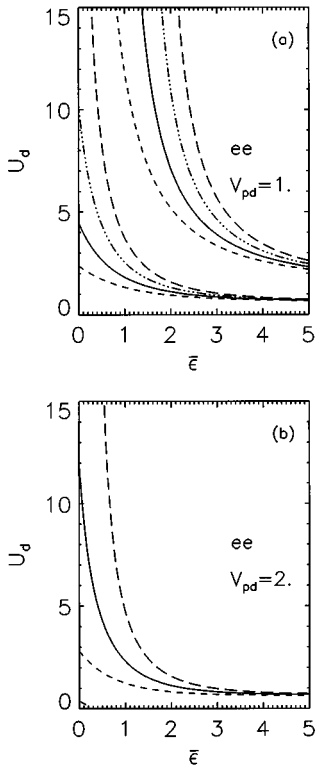


FIG. 17. Boundaries where the static electron-electron interaction $\Delta E^{ee}_{tJV}$ is zero with a paramagnetic background ($V^{ee}-\frac{1}{4}J=0$, left-hand curve) and with an antiferromagnetic background ($V^{ee}-0.585J=0$, right-hand curve): (a) $V_{pd}=1$; $U_p=0$ (long-dashed lines), $U_p=1.5$ (multidot-dashed lines), $U_p=3$ (solid lines), $U_p=4.5$ (dashed lines), (b) $V_{pd}=2$; $U_p=0$ (long-dashed lines), $U_p=2$ (solid lines), $U_p=4$ (dashed lines).

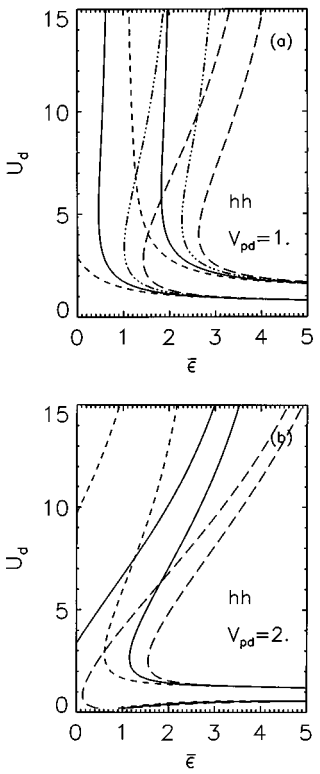


FIG. 18. Boundaries where the static hole-hole interaction $\Delta E^{hh}_{tJV}$ is zero with a paramagnetic background ($V^{hh}-\frac{1}{4}J=0$, left-hand curve) and with an antiferromagnetic background ($V^{hh}-0.585J=0$, right-hand curve); parameter values and curves as in Fig. 17.

around $V_{pd}=2$; i.e., below this value $V_{pd}$ is expected to contribute to repulsion between holes, only reenforcing attraction for $V_{pd}>2$. This maximum shifts to lower $V_{pd}$ with increasing $U_d$, but it is only at considerably larger values of $U_d$ that $V_{pd}$ makes an attractive contribution whenever nonzero. This makes a scenario for superconductive pairing[5] based upon the charge-transfer excitations associated with $V_{pd}$ within the two-band model unlikely for the cuprates and, as mentioned in Sec. III E, shows that setting $U_d=\infty$ can give qualitatively incorrect results.

## V. SUMMARY AND CONCLUSIONS

The purpose of this paper has been to demonstrate that a multi-orbital *d-p* model of copper-oxide planes may be reduced to an effective single-band model over a wide range of parameters and to show explicitly the dependency of effective parameters on those of the underlying *d-p* model. The parameter range has been deliberately extended beyond that expected for the cuprates in order to cover Mott-Hubbard and charge-transfer regimes. This has enabled us to identify the causes of the different behavior in these regimes and to be in a position to ascertain what, if anything, is special about the cuprates. Both electron and hole doping cases have been investigated, enabling us to identify the origins and reasons for different behavior and to discuss the possible consequences. The method and results also provide a unifying theme to a number of apparently disparate approaches to modeling copper-oxide planes and associated physics. It justifies the usual single-band Hubbard model and the *t-J* model, conjectured by Anderson,[1] as the generic model for these systems. It also enables corrections and asymmetry in effective parameters to be justified and computed explicitly. Many of these, such as nearest-neighbor Coulomb interactions[93] and occupation-dependent hopping terms,[94–98] have been incorporated in the Hubbard model in a somewhat *ad hoc* way. Another potentially important effect which has only been investigated directly in terms of the *d-p* model is *d-p* charge polarization, due to copper-oxygen repulsion. This has the potential to give rise to non-Fermi-liquid behavior in the normal state[62–65] and a possible mechanism for superconducting pairing.[5,21,23,51–60] *In the present approach, these effects are completely accounted for in the hopping and (particularly) Coulomb terms in the effective single-band model.*

The main results of this work may be summarized as follows.

(1) For a wide range of parameters a multi-orbital *d-p* model may be accurately reduced to an effective single-band model by a cell perturbation method to second order. This includes Mott-Hubbard and charge-transfer regimes for undoped, electron-doped, and hole-doped cases. The undoped case (or effective half-filled band) includes the metallic regime; i.e., it incorporates the insulator-metal transition. The form of the effective single-band model is the same for all

cases, any differences being only in the magnitudes of the effective parameters and (particularly) their asymmetry.

(2) In all cases we find that *all* the underlying parameters in the $d$-$p$ model are important in determining the effective single-band parameters. Thus, the often used approximations of $U_d=\infty$ and $U_p=t_{pp}=V_{pd}=0$ give significant errors in the effective parameters and their variation with charge-transfer energy ($\varepsilon\equiv\varepsilon_p-\varepsilon_d$).

(3) The behavior in the extreme Mott-Hubbard ($U_d\ll\varepsilon$) and charge-transfer ($U_d\gg\varepsilon$) regimes is quite different. The former reduces to an effective single-band Hubbard model with $U_{\rm eff}\approx U_d$ and $t_{\rm eff}\approx t_{pd}^2/\varepsilon$. As $\varepsilon/U_d$ is decreased and we move towards and into the charge-transfer regime, the effective parameters become increasingly dependent on all the underlying $d$-$p$ parameters and an *appreciable asymmetry between electrons and holes* develops.

(4) In the charge-transfer regime, where $U_{\rm eff}$ is basically the charge-transfer gap, $U_{\rm eff}$ is also quite sensitive to $V_{pd}$ and $U_p$. Then the interplay between $\varepsilon$ and $V_{pd}$ is particularly striking with $U_{\rm eff}$ remaining invariant for a wide range of the ratio $V_{pd}/\varepsilon$. This is potentially very important for the cuprates *since the observed gap may be due to a somewhat larger $V_{pd}$ (and smaller $\varepsilon$) than is generally believed.* This would have a large influence on the effective Coulomb interaction between doped holes. (See below.)

(5) Increasing the Coulomb parameters $V_{pd}$ and $U_p$ will also increase the effective Coulomb interaction between doped electrons and holes on nearest-neighbor cells in most cases. However, in the charge-transfer regime *$V^{hh}$ is reduced with increasing $V_{pd}$*. This is the effective single-band manifestation of the so-called oxygen charge-polarization effect.[5,21,23,51–60] The trend is for the attractive tendency due to $V_{pd}$ to be opposed by $U_p$ and $t_{pp}$ but enhanced by $U_d$. For realistic cuprate parameters we find that the effective hole-hole interaction is *repulsive* and in fact comparable with the corresponding electron-electron interaction (which is always repulsive). However, we emphasize that this small residual repulsion between holes is due to a subtle interplay between the various $d$-$p$ parameters and certain approximations (for example, setting $U_d=\infty$, $U_p=0$, or $t_{pp}=0$) can give the opposite result.

(6) The other main effect of $U_p$ in first-order is to give rise to a ferromagnetic spin-spin interaction which opposes antiferromagnetic superexchange. This can be quite appreciable and its contribution is necessary in order to get reasonable agreement with the observed exchange constant for the cuprates.

(7) The asymmetry in the $ee$, $hh$, and $eh$ nearest-neighbor hopping terms in the effective single-band model can also be quite appreciable with differences up to a factor of 2 between electron and hole hopping. While the magnitudes of these hopping parameters depend sensitively on the underlying $d$-$p$ hopping terms $t_{pp}$ and $t_{pd}$, as expected, the Coulomb parameters are also important and can have a large effect on the asymmetry. It is notable that for the expected parameter range of the cuprates there is, what appears to be, an accidental cancellation of the various contributions which results in *almost perfect electron-hole symmetry* ($t^{ee}\approx t^{hh}$) and only a very small difference between these intraband hopping parameters and the interband $t^{eh}$. This casts some doubt on the viability of occupation-dependent hopping as a mechanism for pairing as proposed by Hirsch and co-workers[94–97] and others.[98]

(8) The *next-nearest-neighbor hopping terms* are particularly sensitive to all the underlying $d$-$p$ parameters and the second-order contributions make a significant, sometimes dominant, contribution. These effective hoppings can be of the same or opposite sign for doped holes or electrons, depending on the underlying parameters. For the cuprates we find that they have the same sign (when the same sign convention, e.g. for holes, is used for both cases), in agreement with earlier findings in small clusters.[10,12] In the context of $t$-$t'$-$J$ models describing either hole doping or electron doping (where it is common practice to use different sign conventions) the signs would therefore be *opposite.* Recently Tohyama and Maekawa[99] have argued that this asymmetry is responsible for the stabilization (destabilization) of antiferromagnetic order for electron doping (hole doping), whereas also the spatial distribution of the doped carriers[100] and the damping of quasiparticles[101] have been shown to be very sensitive to the sign of $t'$. As a small but finite $t'$ is apparently a real feature, since it has been found to be essential in reproducing various experimental observations (magnetic structure factor,[102,103] flat quasiparticle dispersion and shape of the Fermi surface,[104] sign change in the Hall effect,[105]) these findings support the claim[99] that the sign of $t'$ is relevant for the thermodynamics, in agreement with the more general arguments by Lee[106] that the propagation within one sublattice without spin flip allowed by nonzero $t'$ would significantly change the physics. We should, however, point out that the previous estimates based on cluster calculations have probably overestimated the asymmetry, and we find that setting $t'=0$ for electrons is a more accurate approximation than assuming $t'$ to have similar magnitude but opposite sign for electrons and holes. Nevertheless, it is this *electron-hole asymmetry in the next-nearest-neighbor hopping combined with almost perfect symmetry of all other effective parameters* that seems to distinguish the cuprates from a general charge-transfer insulator in the ZSA diagram.

In conclusion, the results of the present investigation leave little doubt that the reduction of a multi-band $d$-$p$ model to an effective single-band model is a valid and tractable problem for a very wide range of $d$-$p$ parameters, also in the presence of Coulomb repulsion on oxygen and between copper and oxygen. The only remaining doubt as to its validity is the effect of extra orbitals not included in the two-band model, since there is always the possibility that these may give rise to cell states which could be sufficiently low in energy that their effect may not be accounted for perturbatively. One possible source of such low-energy cell states is provided by apical oxygen ions with a low-energy $p_z$ orbital. As we show in the companion paper II, with realistic estimates of $d$-$p$ parameters a breakdown of the effective single-band model cannot be ruled out for some materials, though it is unlikely for most of the high-$T_c$ cuprates. Another possible mechanism may be provided by a large copper-oxygen Coulomb repulsion $V_{pd}$ (considerably greater than 2 eV for the cuprates) if the resulting relative lowering of the in-plane oxygen orbitals of $a_1$-symmetry were able to overcome the stabilization of the Zhang-Rice singlet by the $pd$ hybridization. Indeed, Varma and co-workers[64,65] have argued from a different viewpoint that more than one type of

oxygen orbital may be important for the cuprates and instrumental in giving rise to non-Fermi-liquid behavior by a multi-channel Kondo effect. This large $V_{pd}$ regime is difficult to treat by the cell method, though not prohibitively so, and may lead to greater insight into why the effective single-band model might break down and what it could be replaced with. Firm experimental evidence for a large Cu-O repulsive interaction would make an investigation of the cell method into this extended parameter regime worthwhile.

## ACKNOWLEDGMENTS

We would like to thank H. Eskes, A.M. Oleś, M. Grilli, and C. Di Castro for stimulating discussions. This investigation was supported by the European Community under the SCIENCE program for collaborative research [Contract No. SC1*-0222-C(EDB)]. R.R. also acknowledges partial support by the European Union under Contract No. ERB 4050 PL 920925.

[1] P.W. Anderson, Science **235**, 1196 (1987).
[2] V.J. Emery, Phys. Rev. Lett. **58**, 2794 (1987).
[3] P. Kuiper, G. Kruizinga, J. Ghijsen, M. Grioni, G.A. Sawatzky, P.J.W. Weijss, F.H.M. de Groot, H. Verweij, L.F. Feiner, and H. Petersen, Phys. Rev. B **38**, 6483 (1988).
[4] N. Nücker, J. Fink, J.C. Fuggle, P.J. Durham, and W.M. Temmerman, Phys. Rev. B. **37**, 5158 (1988).
[5] C.M. Varma, S. Schmitt-Rink, and E. Abrahams, Solid State Commun. **62**, 681 (1987).
[6] F.C. Zhang and T.M. Rice, Phys. Rev. B **37**, 3757 (1988).
[7] H. Eskes and J.H. Jefferson, Phys. Rev. B **48**, 9788 (1993).
[8] H. Eskes and G.A. Sawatzky, Phys. Rev. Lett. **61**, 1415 (1988).
[9] E.B. Stechel and D.R. Jennison, Phys. Rev. B **38**, 4632 (1988).
[10] H. Eskes, G.A. Sawatzky, and L.F. Feiner, Physica C **160**, 424 (1989).
[11] M.S. Hybertsen, E.B. Stechel, M. Schlüter, and D.R. Jennison, Phys. Rev. B **41**, 11 068 (1990).
[12] T. Tohyama and S. Maekawa, J. Phys. Soc. Jpn. **59**, 1760 (1990).
[13] C.D. Batista and A.A. Aligia, Phys. Rev. B **47**, 8929 (1993).
[14] J.H. Jefferson, H. Eskes, and L.F. Feiner, Phys. Rev. B **45**, 7959 (1992).
[15] S.V. Lovtsov and V.Yu. Yushankhai, Physica C **179**, 159 (1991).
[16] H.-B. Schüttler and A.J. Fedro, Phys. Rev. B **45**, 7588 (1992).
[17] J.H. Jefferson, Physica B **165-166**, 1013 (1990).
[18] A. Moreo and D.J. Scalapino, Phys. Rev. B **43**, 8211 (1991).
[19] E. Dagotto, Rev. Mod. Phys. **66**, 763 (1994).
[20] G. Dopf, A. Muramatsu, and W. Hanke, Phys. Rev. Lett. **68**, 353 (1992).
[21] M. Grilli, R. Raimondi, C. Castellani, C. Di Castro, and G. Kotliar, Phys. Rev. Lett. **67**, 259 (1991); Int. J. Mod. Phys. B **5**, 309 (1991).
[22] Y. Bang, G. Kotliar, R. Raimondi, C. Castellani, and M. Grilli, Phys. Rev. B **47**, 3323 (1993).
[23] R. Raimondi, C. Castellani, M. Grilli, Y. Bang, and G. Kotliar, Phys. Rev. B **47**, 3331 (1993).
[24] R. Hayn, V. Yushankhai, and S. Lovtsov, Phys. Rev. B **47**, 5253 (1993).
[25] M.E. Simón and A.A. Aligia, Phys. Rev. B **52**, 7701 (1995).
[26] A.V. Sherman, Phys. Rev. B **47**, 11 521 (1993).
[27] V.I. Belinicher and A.L. Chernyshev, Phys. Rev. B **49**, 9746 (1994).
[28] V.I. Belinicher, A.L. Chernyshev, and L.V. Popovich, Phys. Rev. B **50**, 13 768 (1994).
[29] M.E. Simón, M. Baliña, and A.A. Aligia, Physica C **206**, 297 (1993).
[30] M.E. Simón and A.A. Aligia, Phys. Rev. B **48**, 7471 (1993).
[31] L.F. Feiner, Phys. Rev. B **48**, 16 857 (1993).
[32] W. Brenig, Phys. Rep. **251**, 153 (1995).
[33] J. Zaanen, G.A. Sawatzky, and J.W. Allen, Phys. Rev. Lett. **55**, 418 (1985).
[34] V.J. Emery and G. Reiter, Phys. Rev. B **38**, 11 938 (1988).
[35] R. Raimondi, L.F. Feiner, and J.H. Jefferson, following paper, Phys. Rev. B **53**, 8774 (1996).
[36] L.F. Feiner, J.H. Jefferson, and R. Raimondi, Phys. Rev. B **51**, 12 797 (1995).
[37] H. Eskes, L.H. Tjeng, and G.A. Sawatzky, Phys. Rev. B **41**, 288 (1990).
[38] M.S. Hybertsen, M. Schlüter, and N.E. Christensen, Phys. Rev. B **39**, 9028 (1989).
[39] A.K. McMahan, R.M. Martin, and S. Satpathy, Phys. Rev. B **38**, 6650 (1988).
[40] A.K. McMahan, J.F. Annett, and R.M. Martin, Phys. Rev. B **42**, 6268 (1990).
[41] J.B. Grant and A.K. McMahan, Phys. Rev. B **46**, 8440 (1992).
[42] B.S. Shastry, Phys. Rev. Lett. **63**, 1288 (1989).
[43] The numerical values of the coefficients, here and below, are for an infinite plane. Equivalent coefficients for a finite system with periodic boundary conditions are calculated in the same way using Fourier summations (see Appendix A of II). The differences are considerable and indicate that significant finite-size effects occur in finite-cluster studies of the three-band model.
[44] The three- and four-site interactions due to the *a* orbitals are, in fact, somewhat larger than those due to the *b* orbitals, since the latter are more confined to the two cells bridged by the oxygen site. This is due, in part, to the choice of canonical fermions which are optimally localized for the *b* orbitals. However, as shown in Ref. 35, the *a* orbitals may be eliminated by perturbation theory, resulting in very weak residual three and four cell interactions.
[45] J. Hubbard, Proc. R. Soc. London A **277**, 237 (1964).
[46] J. Hubbard, Proc. R. Soc. London A **276**, 238 (1963).
[47] Note that the sign convention for all three hopping parameters is that for holes.
[48] H. Eskes, Ph.D. thesis, University of Groningen, 1992.
[49] This is hidden in the cell approach where the Wannier transformation makes the $t_{pd}$ contribution arise formally in first order [compare Eq. (3.3)]. However, the intracell matrix elements in that equation are $\propto t_{pd}/\bar{\varepsilon}$, showing that the contribution to effective hopping is actually $\propto t_{pd}^2/\bar{\varepsilon}$.
[50] For an overview, see C. Di Castro and M. Grilli, in *Phase Separation in Cuprate Superconductors*, edited by E. Sigmund and K.A. Müller (Springer-Verlag, Berlin, 1994), where the connection between phase separation and superconductivity is discussed for correlated electron models in general, including the Hubbard, extended Hubbard, and *t-J* model.

[51] P.B. Littlewood, C.M. Varma, and E. Abrahams, Phys. Rev. Lett. **63**, 2602 (1989).
[52] E.R. Gagliano, A.G. Rojo, C.A. Balseiro, and B. Alascio, Solid State Commun. **64**, 901 (1987).
[53] V.J. Emery and G. Reiter, Phys. Rev. B **38**, 4547 (1988).
[54] J.E. Hirsch, S. Tang, E. Loh, and D.J. Scalapino, Phys. Rev. Lett. **60**, 1668 (1988).
[55] J.E. Hirsch, E. Loh, D.J. Scalapino, and S. Tang, Phys. Rev. B **39**, 243 (1989).
[56] C.A. Balseiro, A.G. Rojo, E.R. Gagliano, and B. Alascio, Phys. Rev. B **38**, 9315 (1988).
[57] M.D. Nuñez Regueiro and A.A. Aligia, Phys. Rev. Lett. **61**, 1889 (1988).
[58] W.H. Stephan, W. van der Linden, and P. Horsch, Phys. Rev. B **39**, 2924 (1989).
[59] J.H. Jefferson, Physica B **163**, 643 (1990).
[60] J. Bała and A.M. Oleś, Phys. Rev. B **47**, 515 (1993).
[61] P.W. Anderson, Phys. Rev. Lett. **64**, 1839 (1990).
[62] C.M. Varma, P.B. Littlewood, S. Schmitt-Rink, E. Abrahams, and A.E. Ruckenstein, Phys. Rev. Lett. **63**, 1996 (1989).
[63] Q. Si and G. Kotliar, Phys. Rev. Lett. **70**, 3143 (1993).
[64] I.E. Perakis, C.M. Varma, and A.E. Ruckenstein, Phys. Rev. Lett. **70**, 3467 (1993).
[65] T. Giamarchi, C.M. Varma, A.E. Ruckenstein, and P. Nozières, Phys. Rev. Lett. **70**, 3967 (1993).
[66] M.B.J. Meinders, L.H. Tjeng, and G.A. Sawatzky, Phys. Rev. Lett. **73**, 2937 (1994).
[67] M.B.J. Meinders, Ph.D. thesis, University of Groningen, 1994.
[68] V.P. Antropov, O. Gunnarson, and O. Jepsen, Phys. Rev. B **46**, 13 647 (1992).
[69] P.A. Brühwiler, A.J. Maxwell, P. Rudolf, C.D. Gutleben, B. Wästberg, and N. Mårtensson, Phys. Rev. Lett. **71**, 3721 (1993).
[70] S. Caprara, C. Di Castro, and M. Grilli, Phys. Rev. B **51**, 9286 (1995).
[71] S. Caprara and M. Grilli, Phys. Rev. B **49**, 6971 (1994).
[72] L.H. Tjeng, J. van Elp, P. Kuiper, and G.A. Sawatzky (unpublished); G.A. Sawatzky, in *Earlier and Recent Aspects of Superconductivity*, edited by G. Bednorz and K.A. Müller, Springer Series in Solid State Sciences Vol. 90 (Springer-Verlag, Berlin, 1990), p. 345.
[73] H. Eskes, M.B.J. Meinders, and G.A. Sawatzky, Phys. Rev. Lett. **67**, 1035 (1991).
[74] M.B.J. Meinders, H. Eskes, and G.A. Sawatzky, Phys. Rev. B **48**, 3916 (1993).
[75] N.F. Mott, *Metal-Insulator Transitions*, (Taylor & Francis, London, 1974), Chap. 4.
[76] J.E. Hirsch, Phys. Rev. Lett. **54**, 1317 (1985).
[77] S.A. Kivelson, V.J. Emery, and H.Q. Lin, Phys. Rev. B **42**, 6523 (1990).
[78] E. Dagotto and J. Riera, Phys. Rev. B **46**, 12 084 (1992).
[79] A. Auerbach and B.E. Larson, Phys. Rev. Lett. **66**, 2262 (1991).
[80] H. Eskes and A.M. Oleś, Phys. Rev. Lett. **73**, 1279 (1994).
[81] H. Eskes, A.M. Oleś, M.B.J. Meinders, and W. Stephan, Phys. Rev. B **50**, 17 980 (1994).
[82] K.B. Lyons, P.A. Fleury, J.P. Remeika, A.S. Cooper, and T.J. Negran, Phys. Rev. B **37**, 2353 (1988).
[83] K.B. Lyons, P.A. Fleury, L.F. Schneemeyer, and J.V. Waszczak, Phys. Rev. Lett. **60**, 732 (1988).
[84] V.J. Emery, S.A. Kivelson, and H.Q. Lin, Phys. Rev. Lett. **64**, 475 (1990).
[85] M. Marder, N. Papanicolau, and G.C. Psaltakis, Phys. Rev. B **41**, 6920 (1990).
[86] C. Castellani, M. Grilli, and G. Kotliar, Phys. Rev. B **43**, 8000 (1991).
[87] M. Grilli, C. Castellani, and G. Kotliar, Phys. Rev. B **45**, 10 805 (1992).
[88] M. Grilli and G. Kotliar, Phys. Rev. Lett. **64**, 1170 (1990).
[89] A. Sudbø and A. Houghton, Phys. Rev. B **42**, 4105 (1990).
[90] A. Moreo, Phys. Rev. B **45**, 4907 (1992).
[91] More precisely, we may define the mean energy per bond as $\Delta E_{tJ}=\langle\Psi_0|\, J(\mathbf{S}_1\cdot\mathbf{S}_2-\frac{1}{4}n_1n_2)|\Psi_0\rangle/P_{12}$, where $|\Psi_0\rangle$ is the ground state of the $t$-$J$ model and $P_{12}\equiv\langle\Psi_0|n_1n_2|\Psi_0\rangle$ is the probability that cells 1 and 2 both contain spins. Thus $\Delta E_{tJ}=J(\langle\mathbf{S}_1\cdot\mathbf{S}_2\rangle-\frac{1}{4})$, where $\langle\mathbf{S}_1\cdot\mathbf{S}_2\rangle\equiv\langle\Psi_0|\mathbf{S}_1\cdot\mathbf{S}_2|\Psi_0\rangle/\langle\Psi_0|n_1n_2|\Psi_0\rangle$. For a phase-separated ground state with true broken symmetry, cells 1 and 2 would be chosen to be in a magnetic region with $P_{12}=1$.
[92] N. Trivedi and D.M. Ceperley, Phys. Rev. B **41**, 4552 (1990).
[93] R. Strack and D. Vollhardt, Phys. Rev. Lett. **70**, 2637 (1993).
[94] J.E. Hirsch, Physica C **158**, 326 (1989); Phys. Lett. A **138**, 83 (1989).
[95] J.E. Hirsch and F. Marsiglio, Phys. Rev. B **39**, 11 515 (1989).
[96] J.E. Hirsch and F. Marsiglio, Phys. Rev. B **41**, 2049 (1990).
[97] F. Marsiglio and J.E. Hirsch, Phys. Rev. B **41**, 6435 (1990).
[98] J. Appel, M. Grodzicki, and F. Paulsen, Phys. Rev. B **47**, 2812 (1993).
[99] T. Tohyama and S. Maekawa, Phys. Rev. B **49**, 3596 (1994).
[100] R.J. Gooding, K.J.E. Vos, and P.W. Leung, Phys. Rev. B **50**, 12 866 (1994).
[101] J. Bała, A.M. Oleś, and J. Zaanen, J. Magn. Magn. Mater. **140-144**, 1939 (1995); Phys. Rev. B **52**, 14 597 (1995).
[102] P. Bénard, L. Chen, and A.-M.S. Tremblay, Phys. Rev. B **47**, 15 217 (1993).
[103] Q. Si, Y. Zha, K. Levin, and J.P. Lu, Phys. Rev. B **47**, 9055 (1993).
[104] D.S. Dessau, Z.-X. Shen, D.M. King, D.S. Marshall, L.W. Lombardo, P.H. Dickinson, A.G. Loeser, J. DiCarlo, A. Kapitulnik, and W.E. Spicer, Phys. Rev. Lett. **71**, 2781 (1993).
[105] E. Dagotto, A. Nazarenko, and M. Boninsegni, Phys. Rev. Lett. **73**, 728 (1994).
[106] P.A. Lee, Phys. Rev. Lett. **63**, 680 (1989).